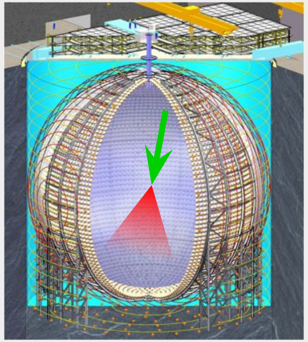

Update on SHELDON laboratory results

JUNO EU-AM collaboration
meeting in Ferrara

Davide Basilico, **Marco Beretta**, Augusto Brigatti, Barbara Caccianiga,
Federico Ferraro, Cecilia Landini, Paolo Lombardi, Alessandra Re, Gioele Reina

Università degli Studi di Milano
INFN-Sezione di Milano

Index

- **The SHELDON project**
- Measurement of fluorescence parameters
- Separation of the Cherenkov contribution
- Evaluation of the Cherenkov contribution
- Conclusion

The SHELDON project: scientific goals

Separation of c**HE**renkov **L**ight for **D**irectionality **O**f **N**eutrino
@ UNIMI - Milan

Two main goals:

Accurate measurement of fluorescence time distribution (fluorescence parameters)

Study of the Cherenkov radiation in the JUNO LS

Impact on the JUNO experiment:

- event reconstruction
- particle identification via PSD
- improved description of fluorescence parameters in the JUNO MC

Impact on the JUNO experiment:

- Improved understanding of energy response
- Possible reconstruction of the direction of incident neutrino

marco.beretta@unimi.it

SHELDON’s laboratory @ UNIMI

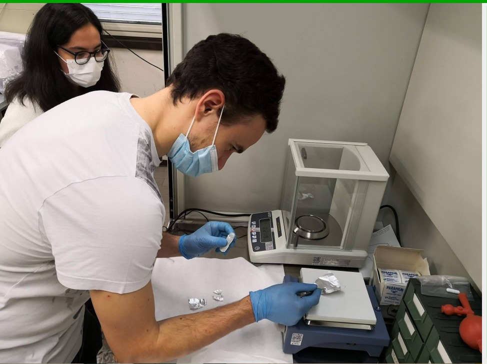

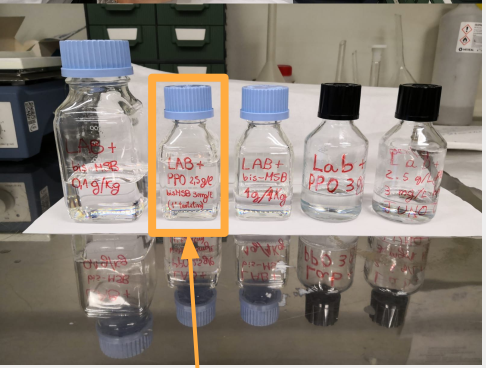

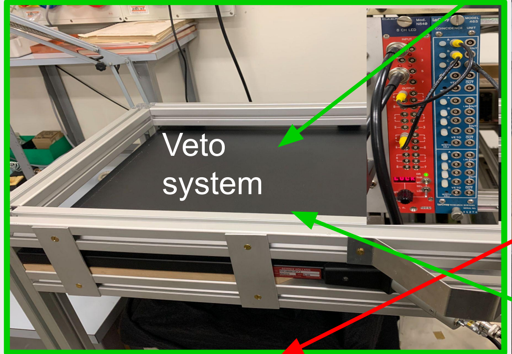

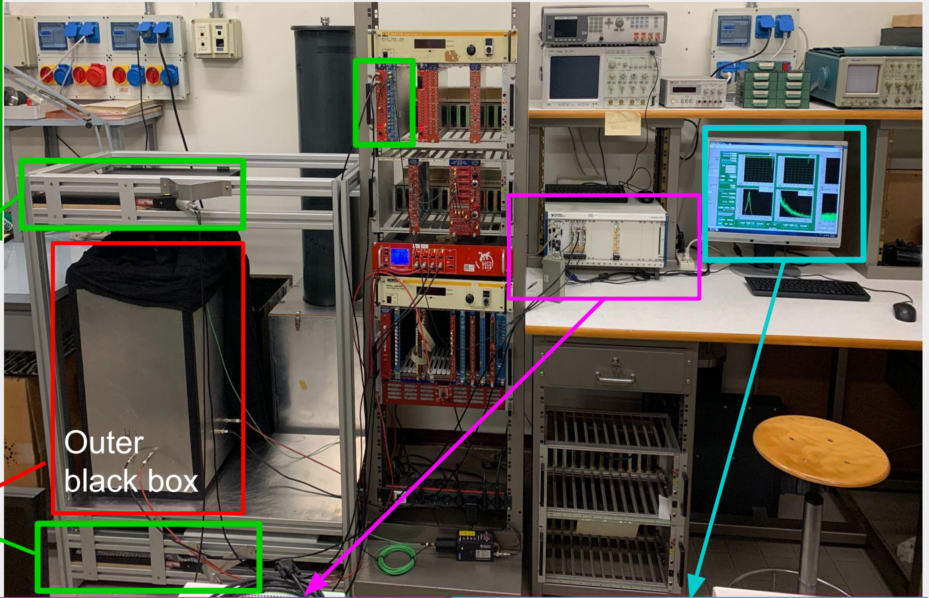

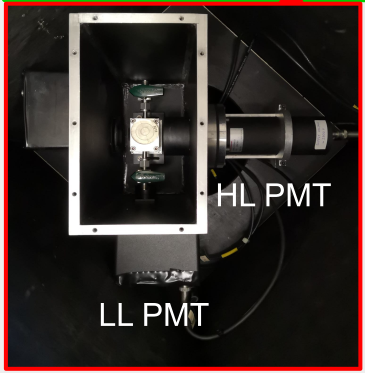

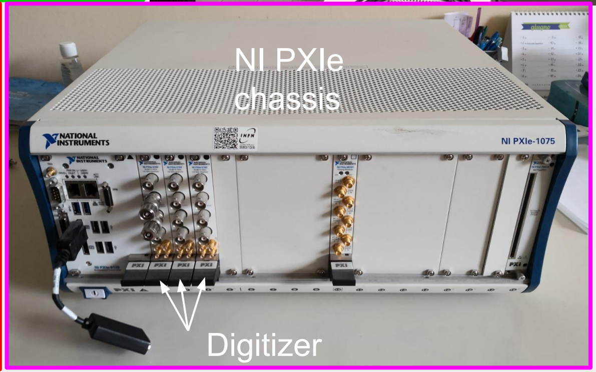

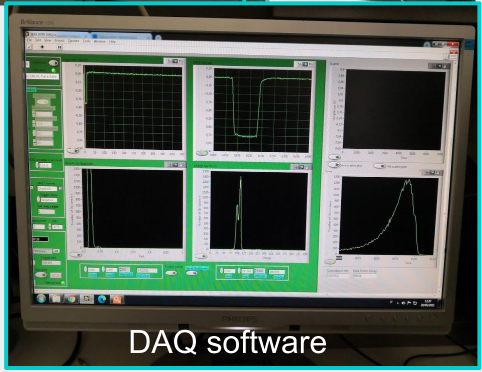

JUNO LS recipe: LAB + 2.5 g/L PPO + 3.0 mg/L bis-MSB

JUNO liquid scintillator: **emission**

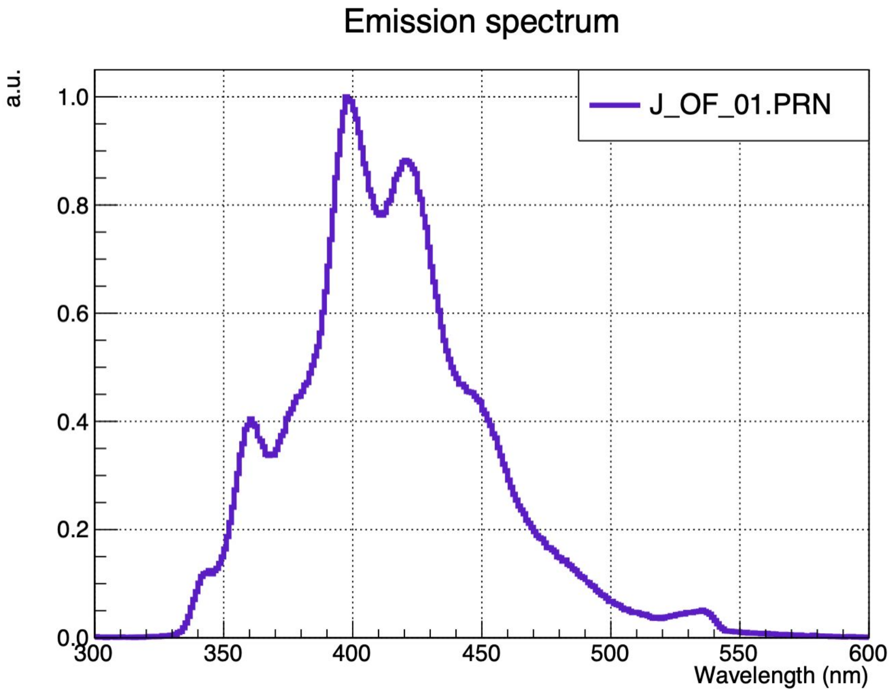

Measured @ Università degli Studi di Perugia
thanks to: Fausto, Aldo e Catia

marco.beretta@unimi.it

JUNO liquid scintillator: **absorption**

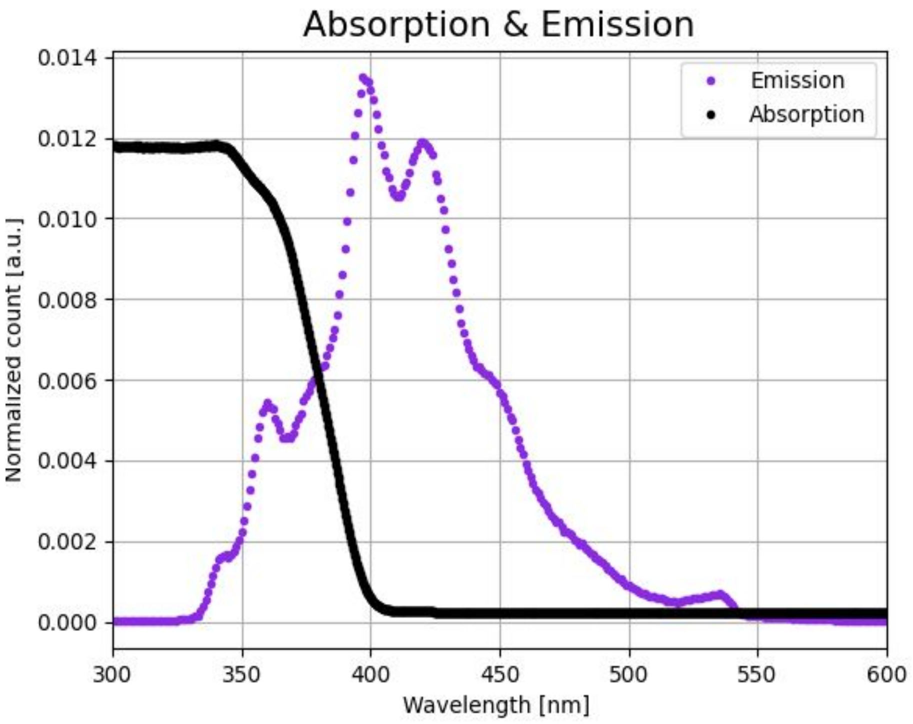

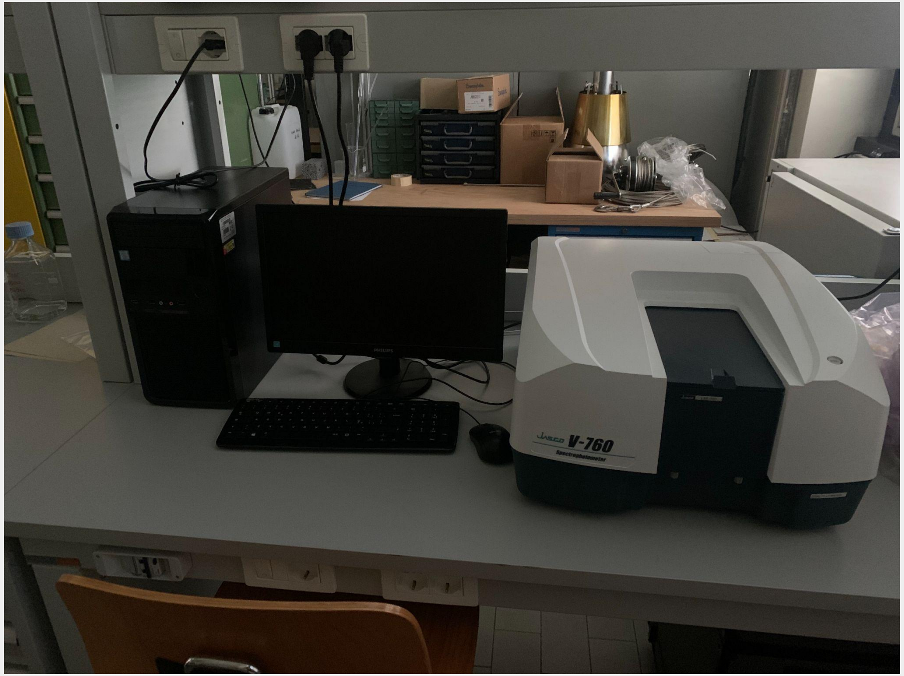

Measured using a spectrophotometer in Milan

marco.beretta@unimi.it

SHELDON: timing measurement setup

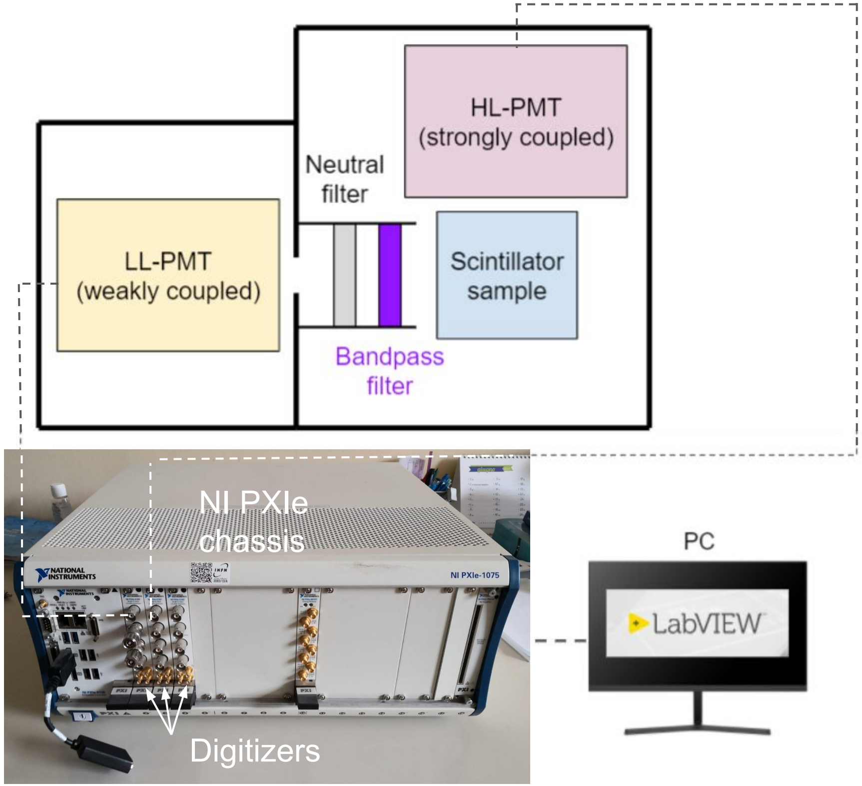

Components of the setup:

JUNO LS sample

2 PMTs, one weakly coupled

Neutral filter

2 Digitizers (5 GS/s each)

LabVIEW DAQ software

Technique:

Time-**C**orrelated **S**ingle **P**hoton **C**ounting

marco.beretta@unimi.it

The SHELDON project: Impulse Response Function

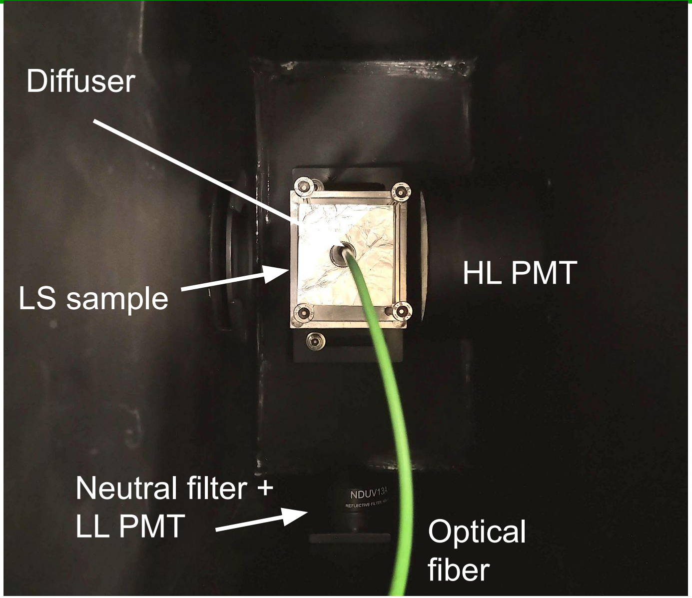

The measurement of the Impulse Response Function (IRF) is performed using a laser.

The laser has a pulse duration of 75 ps.

A diffuser is placed at the end of the optic fibre to mimic a point like emission

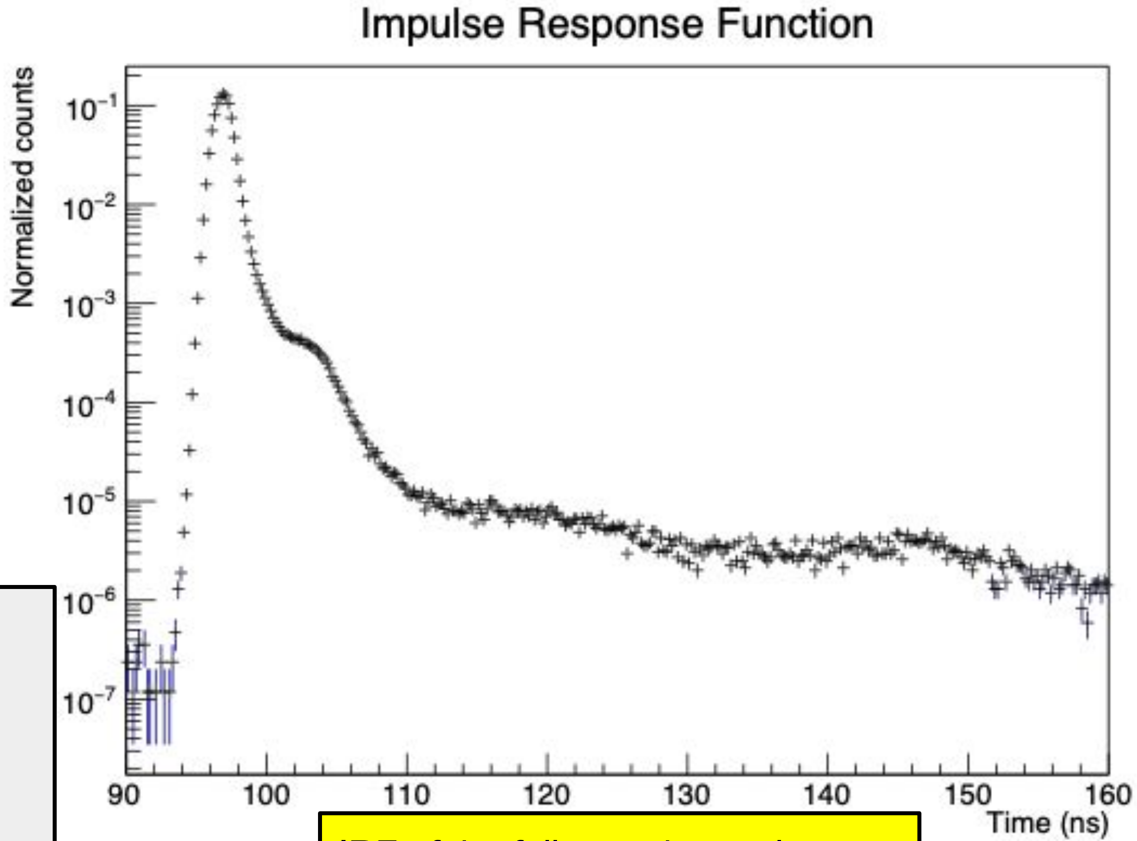

IRF of the full experimental setup:
LS + PMT + ADC + CFD

SHELDON: veto system

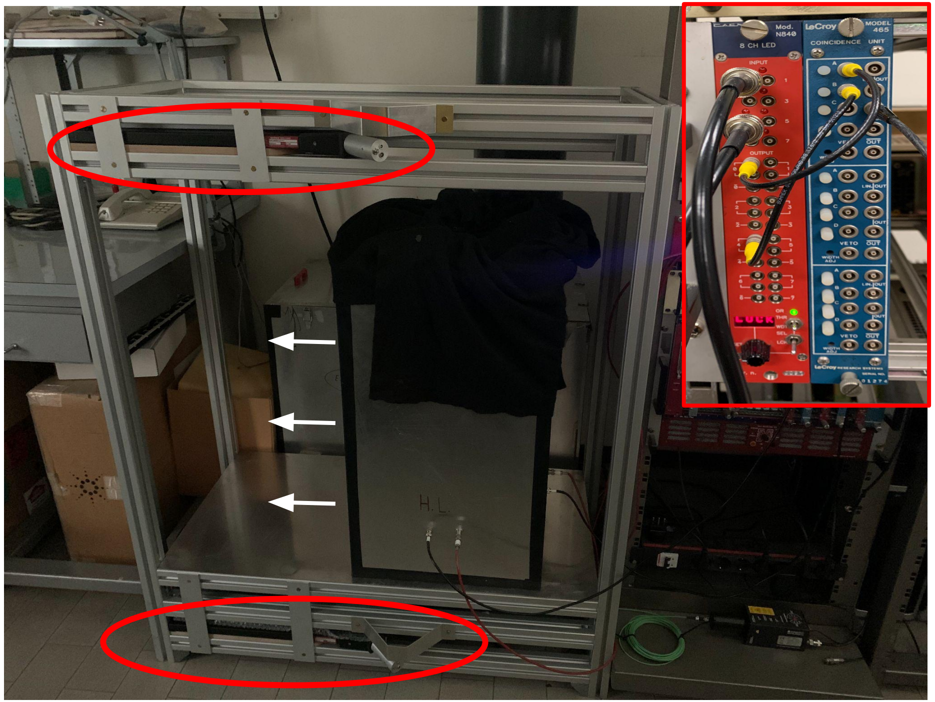

Components of the setup:

2 plastic scintillators EJ 200

Linear Edge Discriminator

Coincidence Unit

3rd Digitizer (5 GS/s)

Same LabVIEW DAQ software

Delay in delivery of components → installed in the last two weeks

marco.beretta@unimi.it

Index

- The SHELDON project
- **Measurement of fluorescence parameters**
- Separation of the Cherenkov contribution
- Evaluation of the Cherenkov contribution
- Conclusion

Measurement of fluorescence

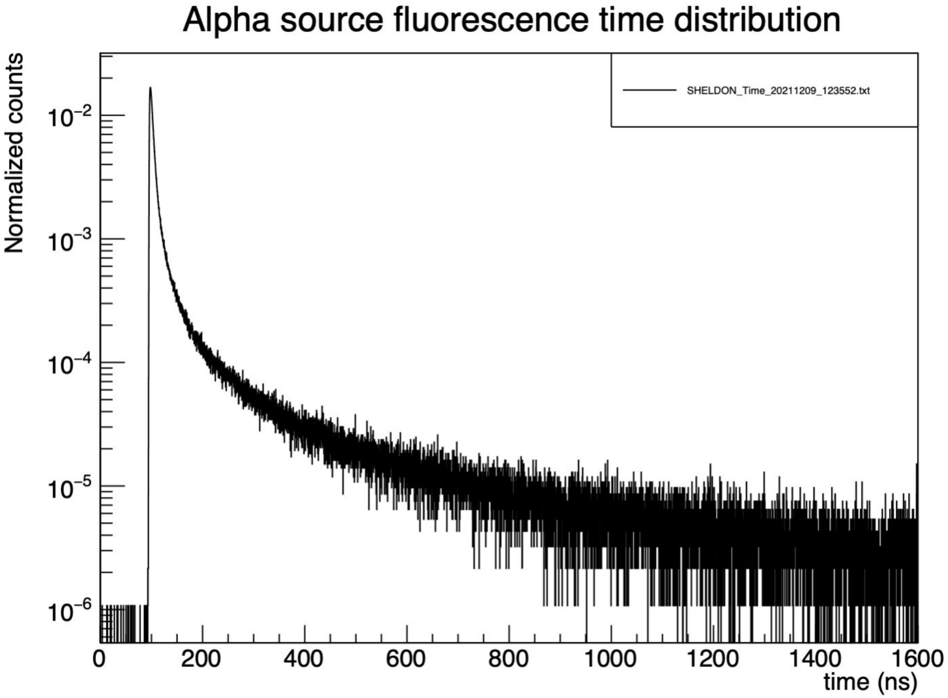

Fluorescence time distribution obtained using an alpha source

Same experimental setup used in the IRF measurement

The duration of the data acquisition is 10 days to obtain 10^6 events

The light emission is **not** a prompt emission

marco.beretta@unimi.it

Fit model: four exponential decay

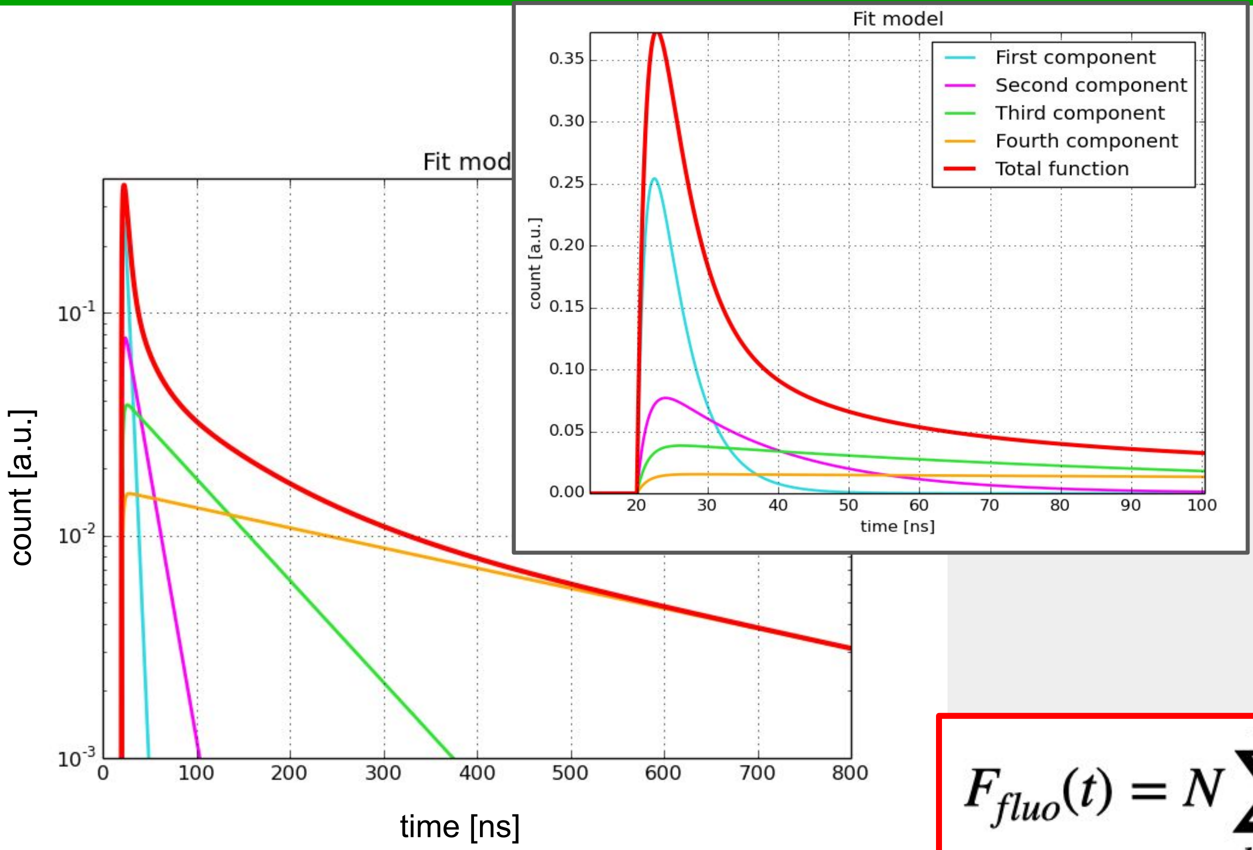

To describe the fluorescence time profile **4 components** are needed

The fourth becomes dominant starting from **~300 ns**

Our DAQ time window is **1600 ns**

$$F_{fluo}(t) = N \sum_{d=1}^{4} \frac{q_d}{\tau_d - \tau_r} \left(e^{-t/\tau_d} - e^{-t/\tau_r} \right)$$

marco.beretta@unimi.it

Measurement of fluorescence parameters: α-source

without veto system

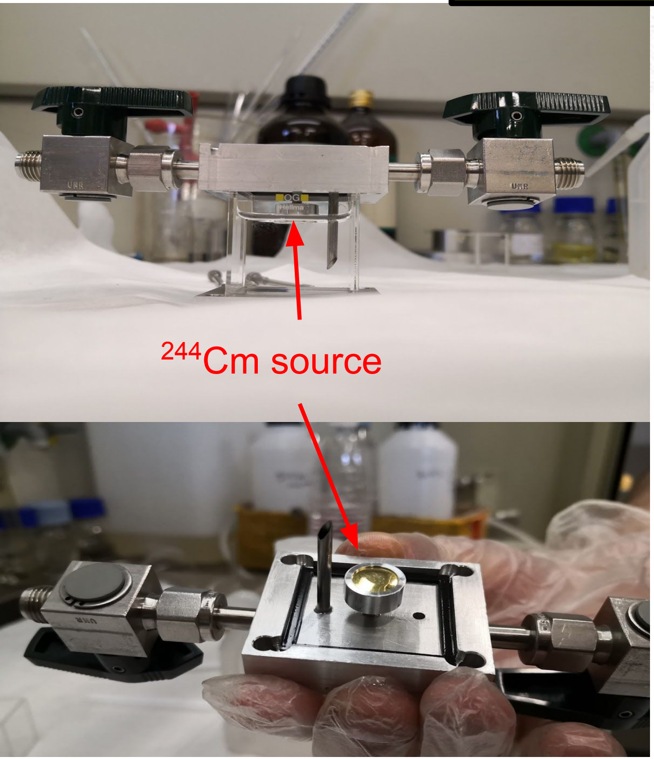

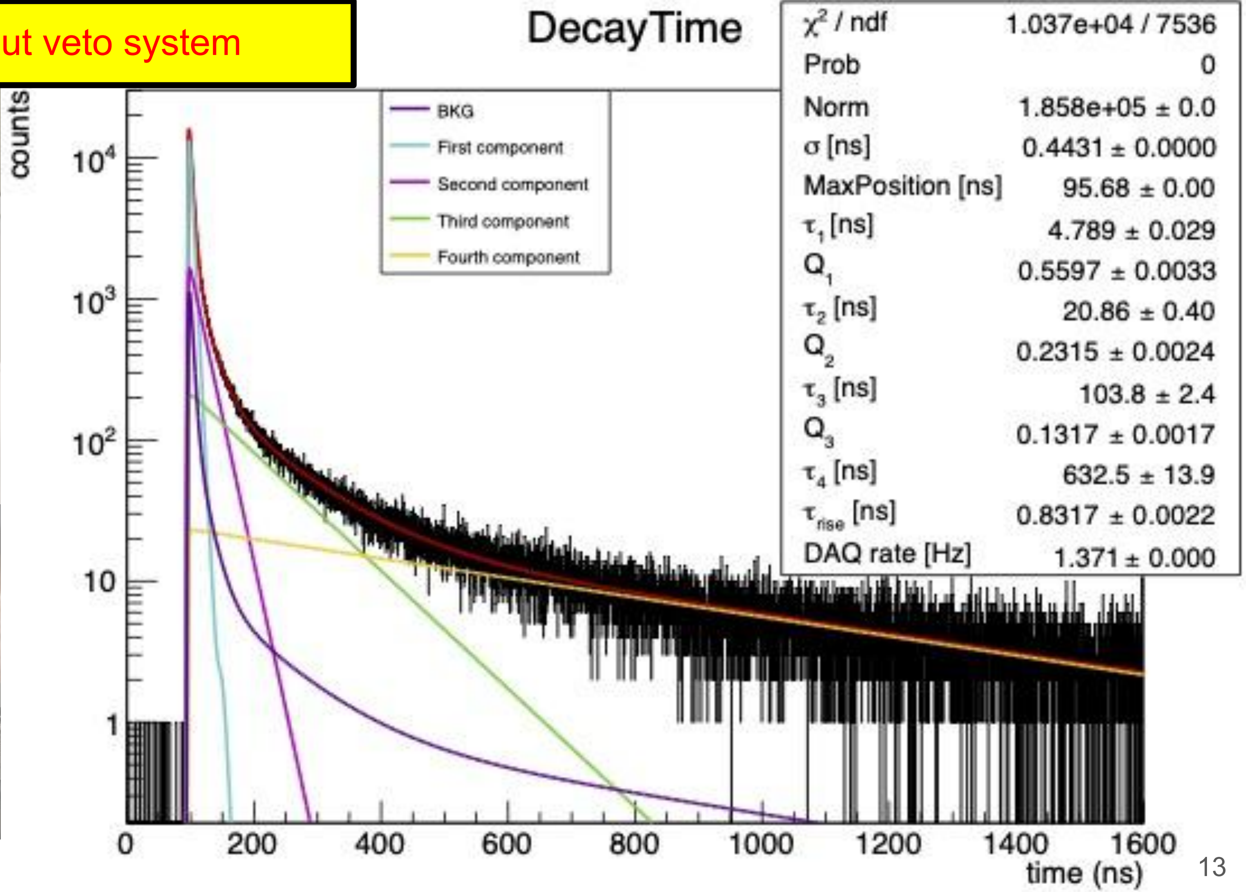

marco.beretta@unimi.it

Measurement of fluorescence parameters: α-source

without veto system

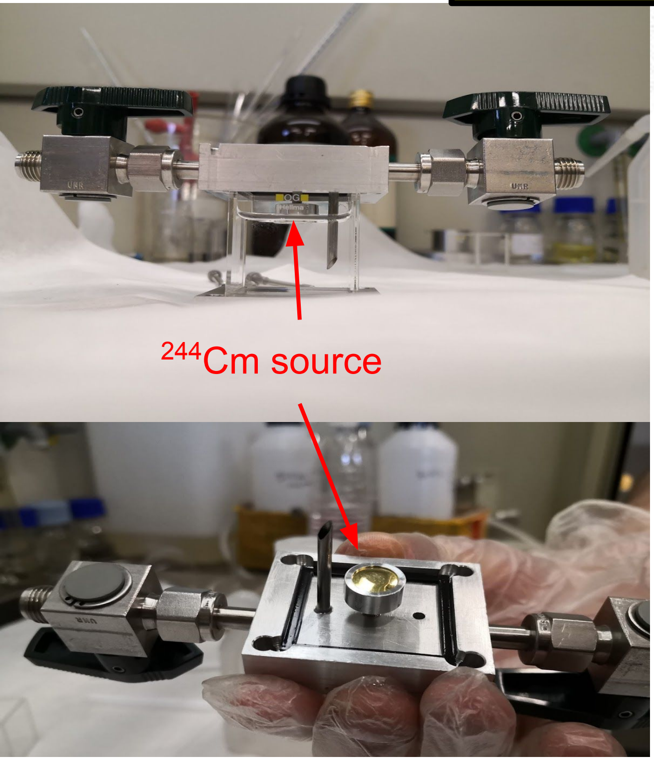

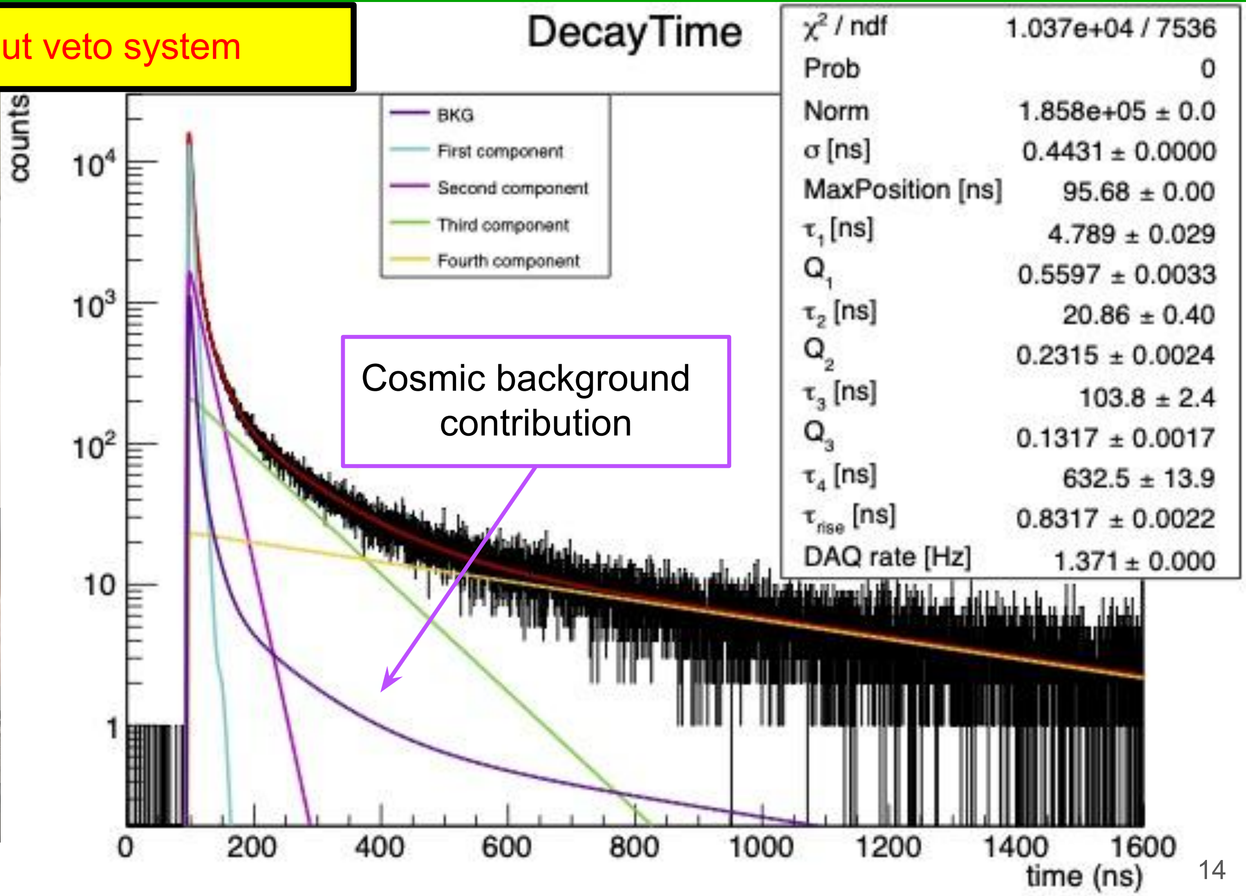

marco.beretta@unimi.it

Measurement of fluorescence parameters: α-source

veto system

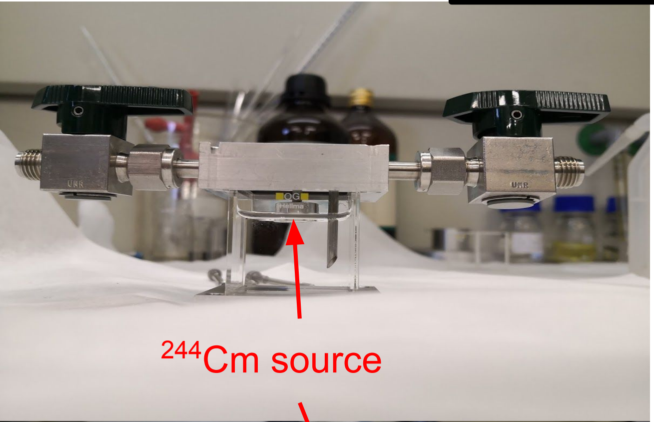

^{244}Cm source

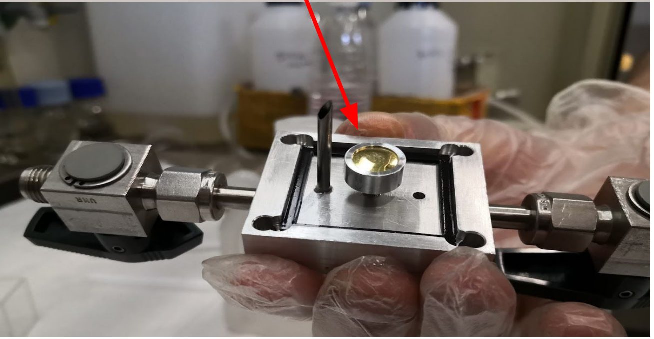

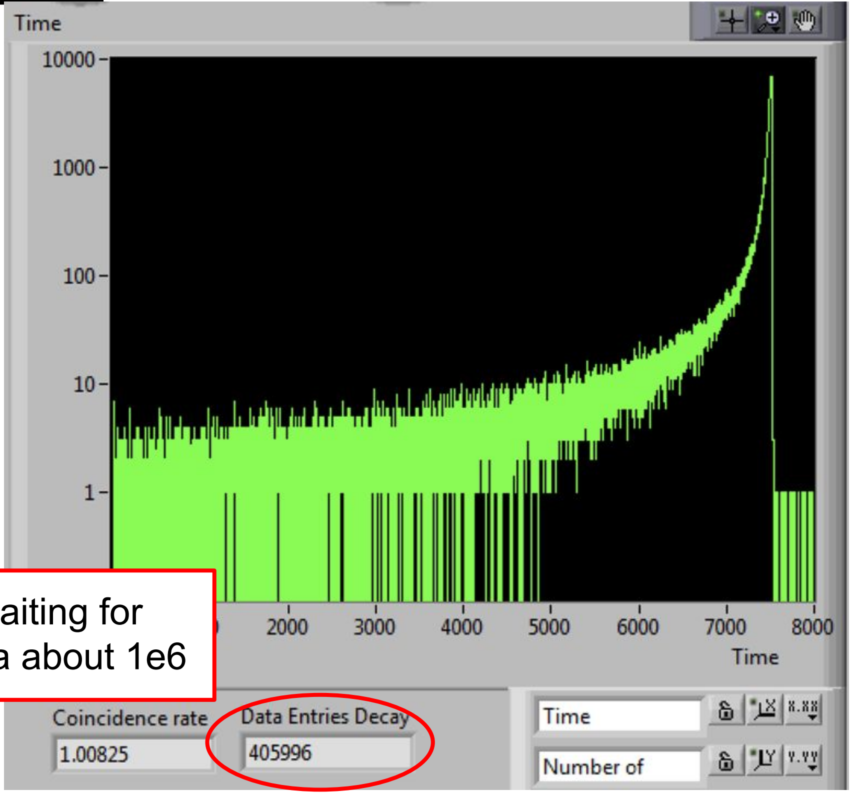

We are waiting for more data about 1e6

marco.beretta@unimi.it

Measurement of fluorescence: preliminary results

without veto system

Measurement of **fluorescence time distribution** using three different radioactive sources.

The three curves have different tails.

We can study how our parameters impact on the JUNO MC simulation
-> **Marco Malabarba's talk**

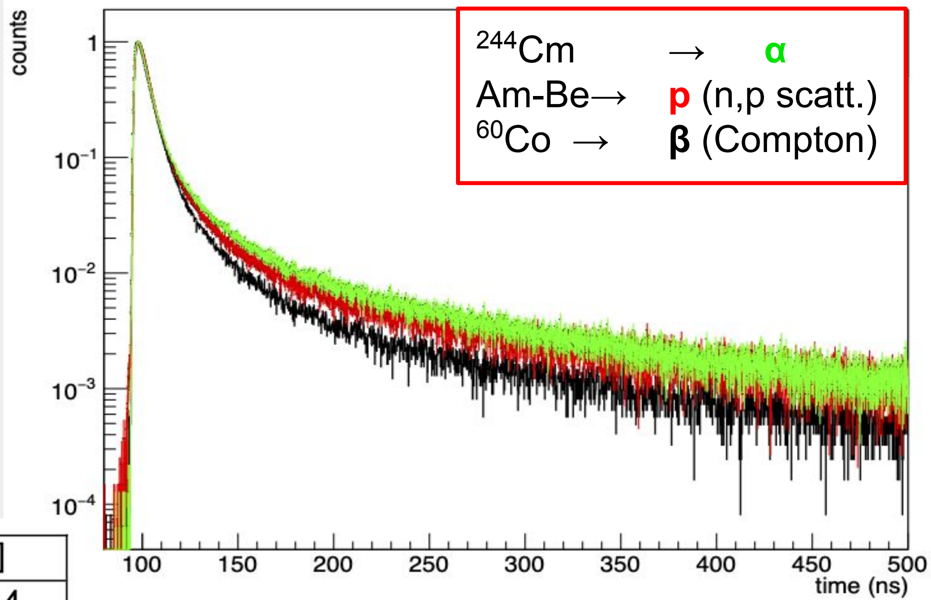

	τ_1 [ns]	τ_2 [ns]	τ_3 [ns]	τ_4 [ns]
α	4.79 ± 0.02	20.86 ± 0.39	103.8 ± 2.4	633 ± 14
p	4.60 ± 0.02	18.99 ±0.27	108.2 ± 2.1	691 ± 12
e^-	3.96 ± 0.02	15.11 ± 0.22	85.0 ± 2.0	549 ± 9
	q_1 [%]	q_2 [%]	q_3 [%]	q_4 [%]
α	55.97 ± 0.32	23.15 ± 0.23	13.17 ± 0.16	8.50 ± 0.42
p	62.02 ± 0.27	21.07 ± 0.21	9.94 ± 0.10	6.97 ± 0.36
e^-	65.02 ± 0.36	23.72 ± 0.28	7.26 ± 0.10	4.27 ± 0.47

WITHOUT VETO PRELIMINARY RESULTS

marco.beretta@unimi.it

Measurement of fluorescence: preliminary results

without veto system

Measurement of **fluorescence time distribution** using three different radioactive sources.

The three curves have different tails.

We can study how our parameters impact on the JUNO MC simulation
-> **Marco Malabarba's talk**

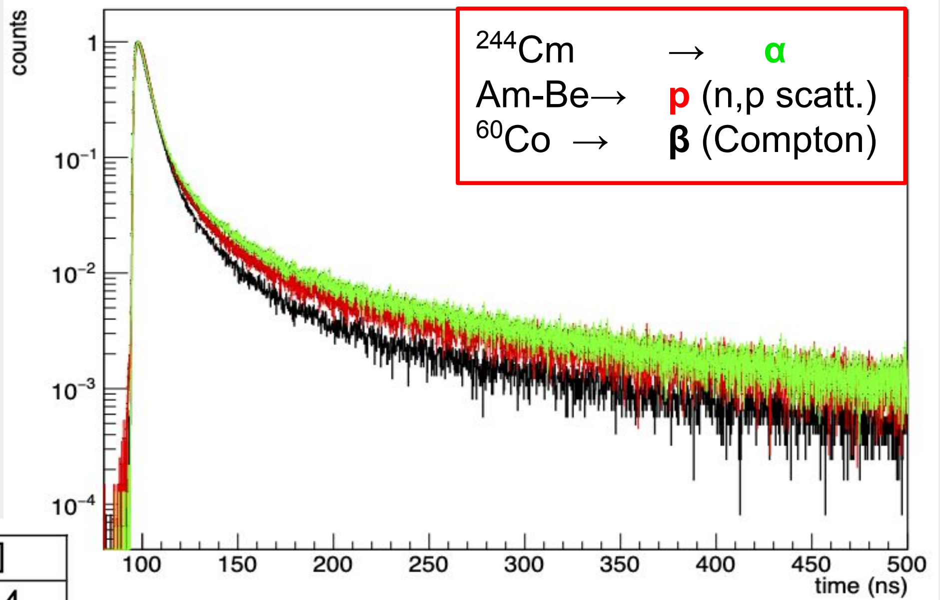

	τ_1 [ns]	τ_2 [ns]	τ_3 [ns]	τ_4 [ns]
α	4.79 ± 0.02	20.86 ± 0.39	103.8 ± 2.4	633 ± 14
p	4.60 ± 0.02	18.99 ±0.27	108.2 ± 2.1	691 ± 12
e^-	3.96 ± 0.02	15.11 ± 0.22	85.0 ± 2.0	549 ± 9
	q_1 [%]	q_2 [%]	q_3 [%]	q_4 [%]
α	55.97 ± 0.32	23.15 ± 0.23	13.17 ± 0.16	8.50 ± 0.42
p	62.02 ± 0.27	21.07 ± 0.21	9.94 ± 0.10	6.97 ± 0.36
e^-	65.02 ± 0.36	23.72 ± 0.28	7.26 ± 0.10	4.27 ± 0.47

WITHOUT VETO PRELIMINARY RESULTS

We started the measurement campain with veto and then we will share final results to the collaboration.

marco.beretta@unimi.it

Index

- The SHELDON project
- Measurement of fluorescence parameters
- **Separation of the Cherenkov contribution**
- Evaluation of the Cherenkov contribution
- Conclusion

Cherenkov contribution at different wavelengths

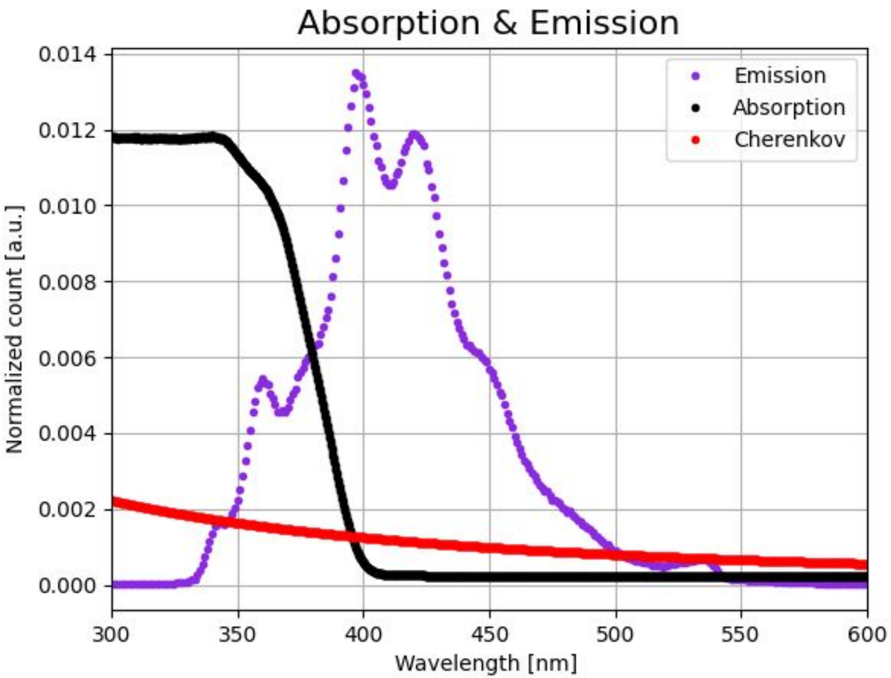

Cherenkov light can be separated from scintillation light thanks to its spectral features.

The JUNO LS emission spectrum has a maximum at 400 nm

The Cherenkov spectrum (not to scale) decreases as $1/\lambda^2$ and extends above the scintillation spectrum.

Using appropriate optical filters it is possible to select the light in a **desired wavelength interval,** separating scintillation and Cherenkov light.

marco.beretta@unimi.it

Cherenkov contribution at different wavelengths

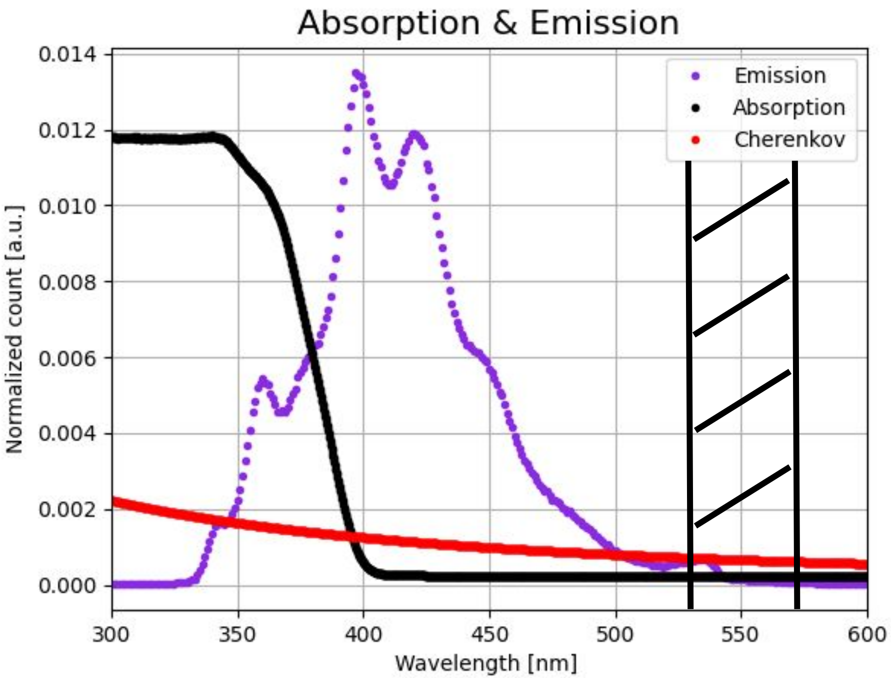

550 - 40 nm

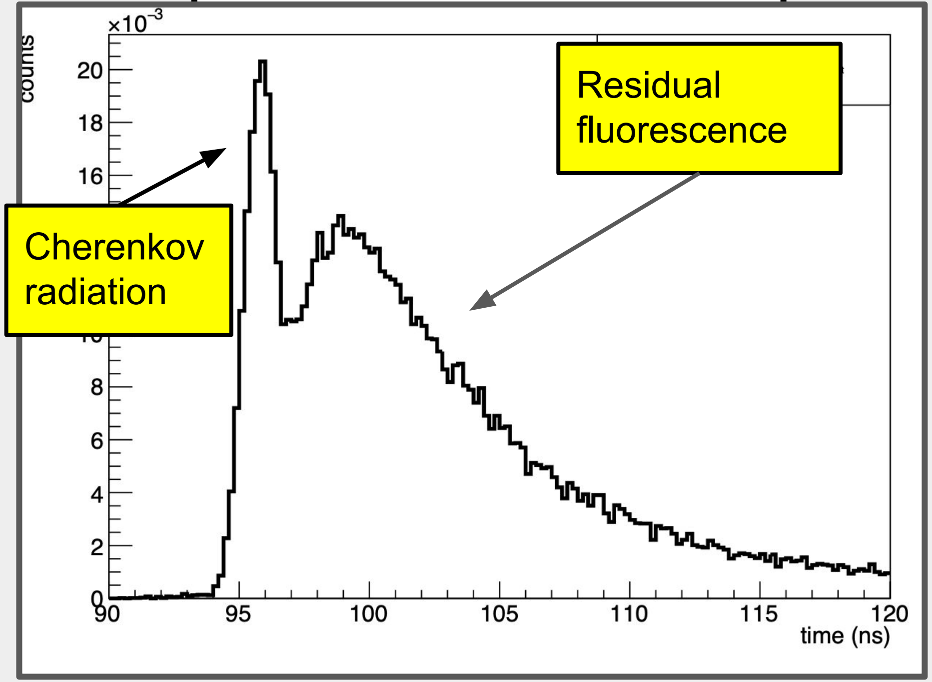

marco.beretta@unimi.it

Cherenkov contribution at different wavelengths

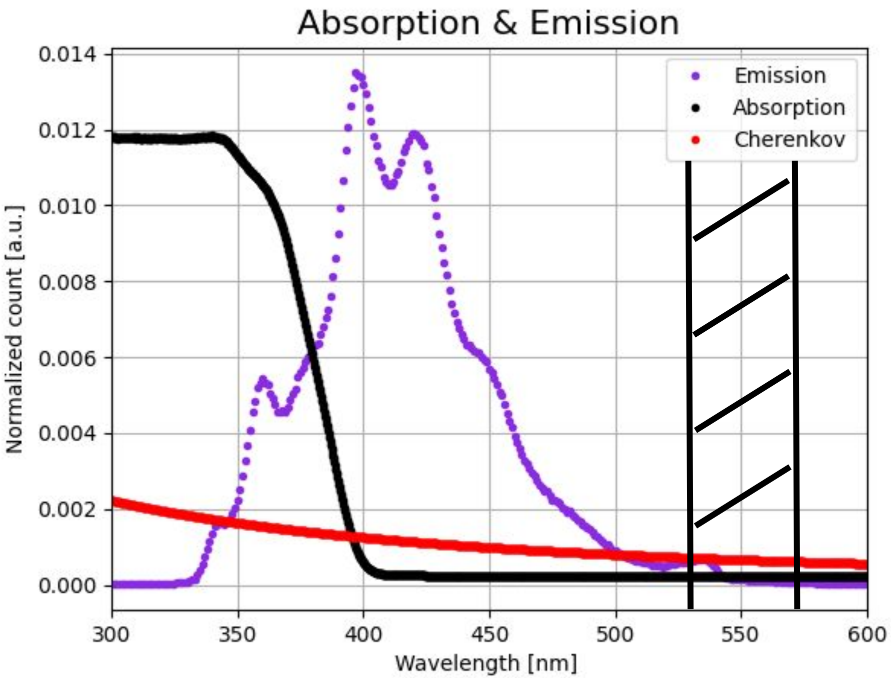

550 - 40 nm

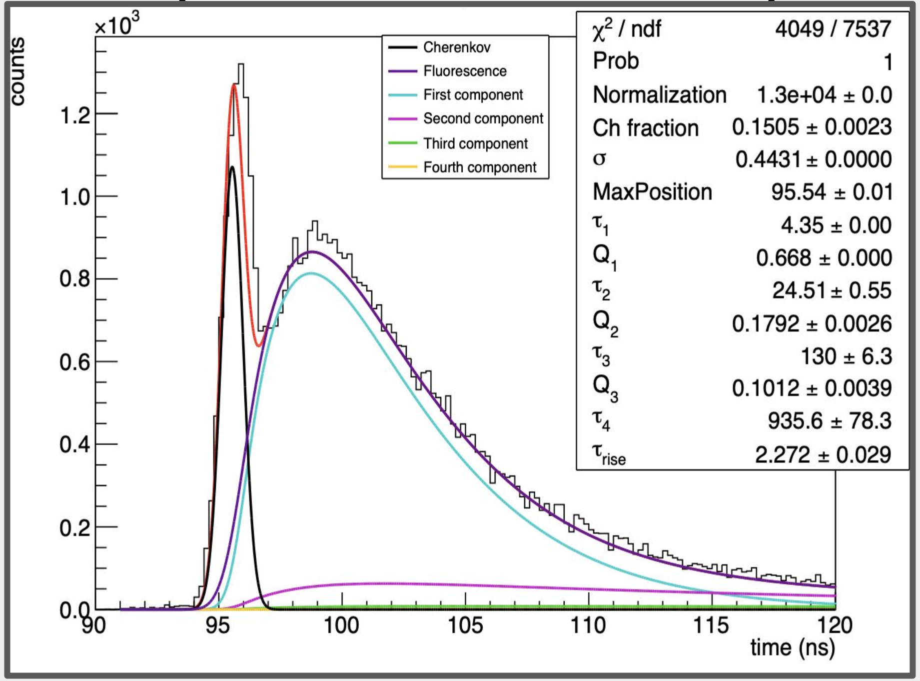

Cherenkov = 15.1 ± 0.2 %

marco.beretta@unimi.it

Index

- The SHELDON project
- Measurement of fluorescence parameters
- Separation of the Cherenkov contribution
- **Evaluation of the Cherenkov contribution**
- Conclusion

Evaluation of the Cherenkov contribution

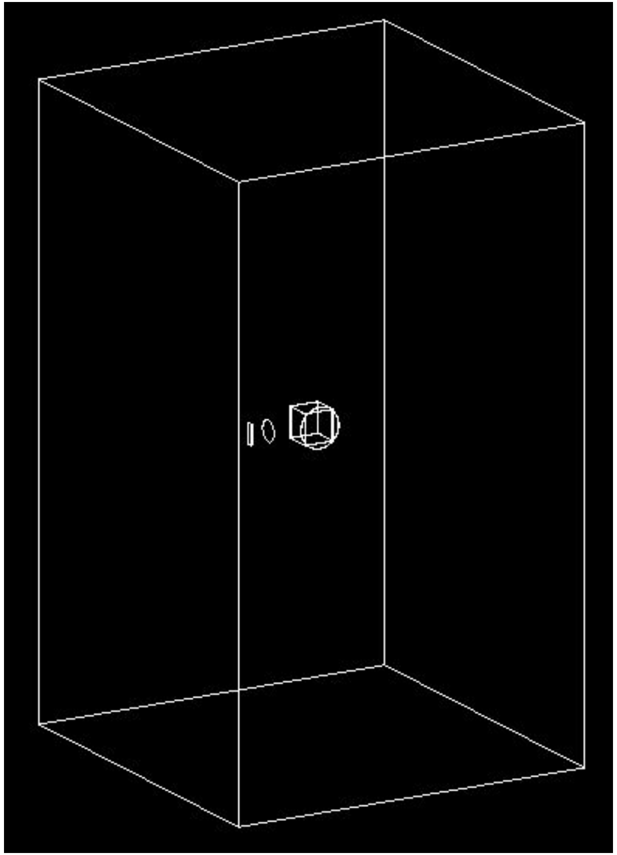

Using the new measurement of the **refractive index**

-> Gioele Reina's Talk

And a Geant4 simulation of our setup developed by Gioele Reina (master student @ UNIMI)

marco.beretta@unimi.it

Evaluation of the Cherenkov contribution

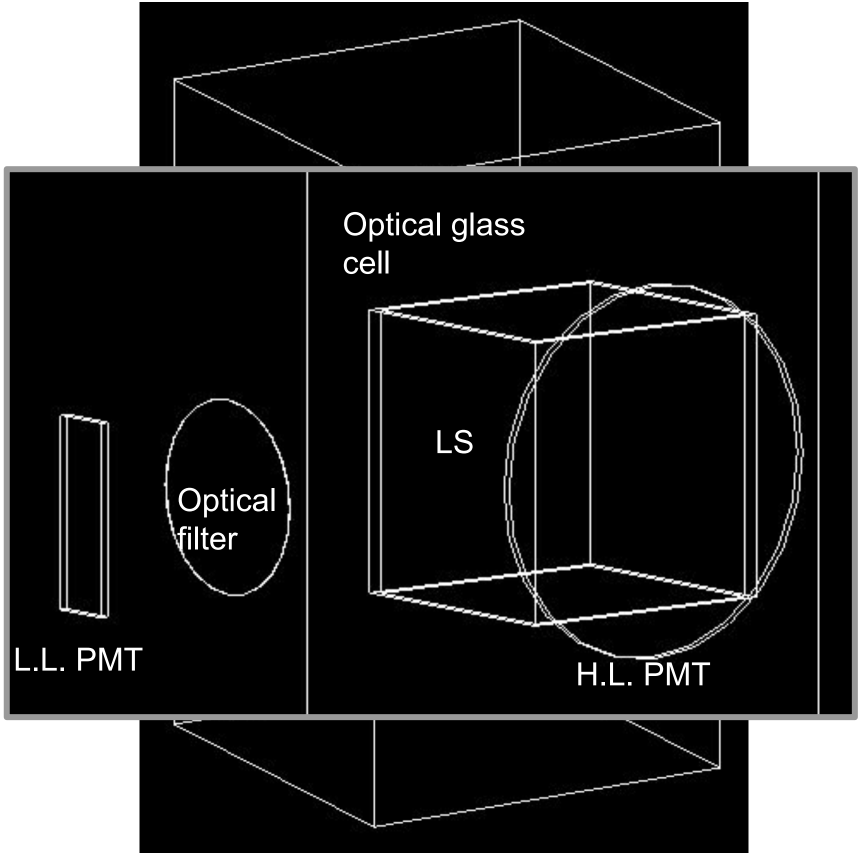

Using the new measurement of the **refractive index**

-> Gioele Reina's Talk

And a Geant4 simulation of our setup developed by Gioele Reina (master student @ UNIMI)

marco.beretta@unimi.it

Evaluation of the Cherenkov contribution

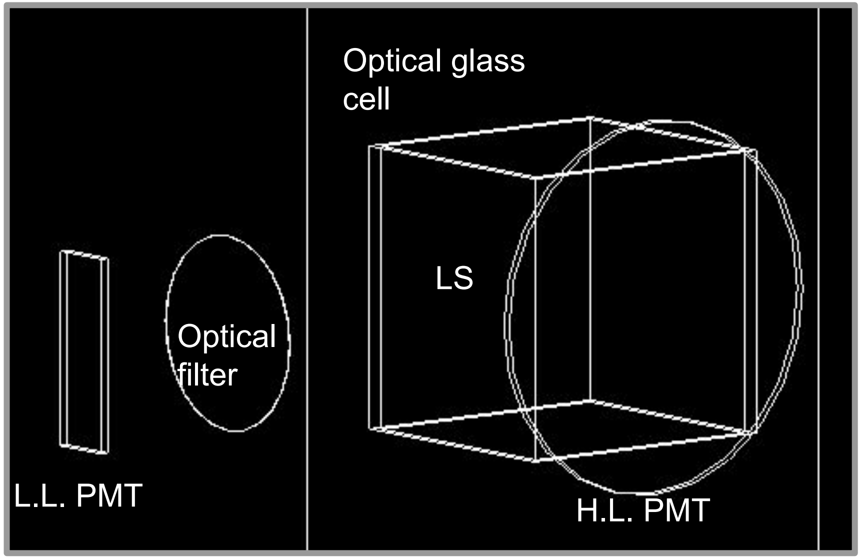

550 - 40 nm

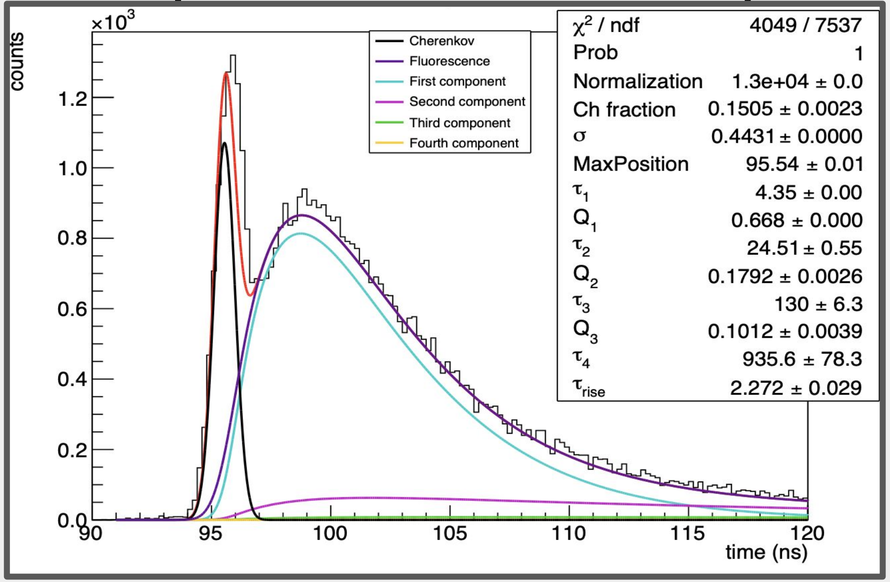

We will measure the Cherenkov contribution in the JUNO LS comparing real data with simulations

marco.beretta@unimi.it

Index

- The SHELDON project
- Measurement of fluorescence parameters
- Separation of the Cherenkov contribution
- Evaluation of the Cherenkov contribution
- **Conclusion**

Conclusions (1)

- We developed an experimental setup for the fluorescence time measurement
- We produced the JUNO liquid scintillator and measured the emission spectrum
- We measured the fluorescence distribution with three radioactive sources
- We are improved the setup with a muon veto
- We are measuring the Cherenkov contribution at different wavelength

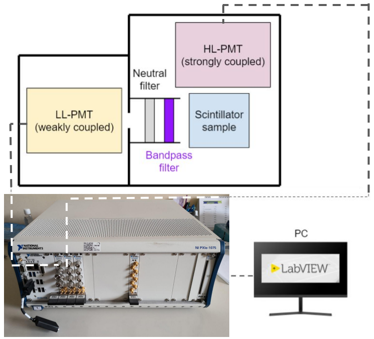

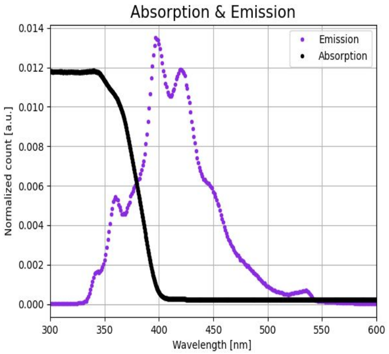

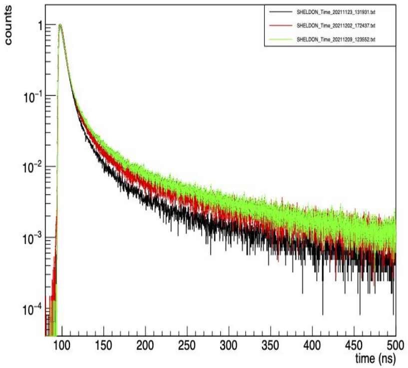

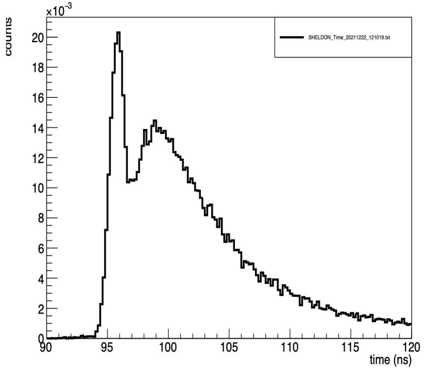

marco.beretta@unimi.it

Conclusions (2)

- we stress the need of creating a database with the different sets of parameters and an ID for each set (to be included in SNIPER) → talk to AFG soon
- we will discuss the consistency of our analysis with other people involved in similar measurements → during this meeting
- we plan to finalize a paper on this measurements → in the very next weeks

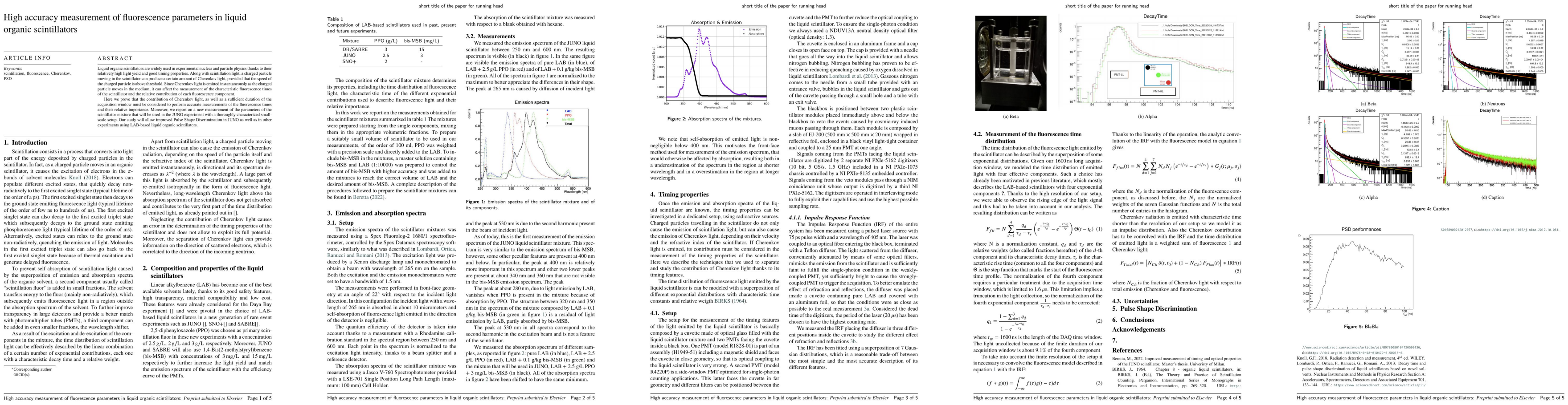

High accuracy measurement of fluorescence parameters in liquid organic scintillators

ARTICLE INFO

Keywords:
scintillation, fluorescence, Cherenkov, PSD

ABSTRACT

Liquid organic scintillators are widely used in experimental nuclear and particle physics thanks to their relatively high light yield and good timing properties. Along with scintillation light, a charged particle moving in the scintillator can produce a certain amount of Cherenkov light, provided that the speed of the charged particle is above threshold. Since Cherenkov light is emitted instantaneously as the charged particle moves in the medium, it can affect the measurement of the characteristic fluorescence times of the scintillator and the relative contribution of each fluorescence component.

Here we prove that the contribution of Cherenkov light, as well as a sufficient duration of the acquisition window must be considered to perform accurate measurements of the fluorescence times and their relative importance. Moreover, we report on a new measurement of the parameters of the scintillator mixture that will be used in the JUNO experiment with a thoroughly characterized small-scale setup. Our study will allow improved Pulse Shape Discrimination in JUNO as well as in other experiments using LAB-based liquid organic scintillators.

1. Introduction

Scintillation consists in a process that converts into light part of the energy deposited by charged particles in the scintillator. In fact, as a charged particle moves in an organic scintillator, it causes the excitation of electrons in the π-bonds of solvent molecules Knoll (2018). Electrons can populate different excited states, that quickly decay non-radiatively to the first excited singlet state (typical lifetime of the order of a ps). The first excited singlet state then decays to the ground state emitting fluorescence light (typical lifetime of the order of few ns to hundreds of ns). The first excited singlet state can also decay to the first excited triplet state which subsequently decays to the ground state emitting phosphorescence light (typical lifetime of the order of ms). Alternatively, excited states can relax to the ground state non-radiatively, quenching the emission of light. Molecules in the first excited triplet state can also go back to the first excited singlet state because of thermal excitation and generate delayed fluorescence.

To prevent self-absorption of scintillation light caused by the superposition of emission and absorption spectra of the organic solvent, a second component usually called "scintillation fluor" is added in small fractions. The solvent transfers energy to the fluor (mainly non-radiatively), which subsequently emits fluorescence light in a region outside the absorption spectrum of the solvent. To further improve transparency in large detectors and provide a better match with photomultiplier tubes (PMTs), a third component can be added in even smaller fractions, the wavelength shifter.

As a result of the excitation and de-excitation of the components in the mixture, the time distribution of scintillation light can be effectively described by the linear combination of a certain number of exponential contributions, each one with a characteristic decay time and a relative weight.

*Corresponding author
ORCID(s):

Apart from scintillation light, a charged particle moving in the scintillator can also cause the emission of Cherenkov radiation, depending on the speed of the particle itself and the refractive index of the scintillator. Cherenkov light is emitted instantaneously, is directional and its spectrum decreases as λ^{-2} (where λ is the wavelength). A large part of this light is absorbed by the scintillator and subsequently re-emitted isotropically in the form of fluorescence light. Nevertheless, long-wavelength Cherenkov light above the absorption spectrum of the scintillator does not get absorbed and contributes to the very first part of the time distribution of emitted light, as already pointed out in [].

Neglecting the contribution of Cherenkov light causes an error in the determination of the timing properties of the scintillator and does not allow to exploit its full potential. Moreover, the separation of Cherenkov light can provide information on the direction of scattered electrons, which is correlated to the direction of the incoming neutrino.

2. Composition and properties of the liquid scintillators

Linear alkylbenzene (LAB) has become one of the best available solvents lately, thanks to its good safety features, high transparency, material compatibility and low cost. These features were already considered for the Daya Bay experiment [] and were pivotal in the choice of LAB-based liquid scintillators in a new generation of rare event experiments such as JUNO [], SNO+[] and SABRE[].

2,5-diphenyloxazole (PPO) was chosen as primary scintillation fluor in these new experiments with a concentration of 2.5 g/L, 2 g/L and 3 g/L respectively. Moreover, JUNO and SABRE will also use 1,4-Bis(2-methylstyryl)benzene (bis-MSB) with concentrations of 3 mg/L and 15 mg/L respectively to further increase the light yield and match the emission spectrum of the scintillator with the efficiency curve of the PMTs.

Table 1
Composition of LAB-based scintillators used in past, present and future experiments.

Mixture	PPO (g/L)	bis-MSB (mg/L)
DB/SABRE	3	15
JUNO	2.5	3
SNO+	2	-

The composition of the scintillator mixture determines its properties, including the time distribution of fluorescence light, the characteristic time of the different exponential contributions used to describe fluorescence light and their relative importance.

In this work we report on the measurements obtained for the scintillator mixtures summarized in table 1 The mixtures were prepared starting from the single components, mixing them in the appropriate volumetric fractions. To prepare a suitably small volume of scintillator to be used in our measurements, of the order of 100 ml, PPO was weighted with a precision scale and directly added to the LAB. To include bis-MSB in the mixtures, a master solution containing bis-MSB and LAB (1:10000) was prepared to control the amount of bis-MSB with higher accuracy and was added to the mixtures to reach the correct volume of LAB and the desired amount of bis-MSB. A complete description of the procedures followed to prepare the scintillator mixtures can be found in Beretta (2022).

3. Emission and absorption spectra

3.1. Setup

The emission spectra of the scintillator mixtures was measured using a Spex Fluorolog-2 1680/1 spectrofluorimeter, controlled by the Spex Datamax spectroscopy software, similarly to what was described in Lombardi, Ortica, Ranucci and Romani (2013). The excitation light was produced by a Xenon discharge lamp and monochromated to obtain a beam with wavelength of 265 nm on the sample. Both the excitation and the emission monochromators were set to have a bandwidth of 1.5 nm.

The measurements were performed in front-face geometry at an angle of 22° with respect to the incident light direction. In this configuration the incident light with a wavelength of 265 nm is absorbed in about 10 micrometers and self-absorption of fluorescence light emitted in the direction of the detector is negligible.

The quantum efficiency of the detector is taken into account thanks to a measurement with a Rhodamine calibration standard in the spectral region between 250 nm and 600 nm. Each point in the spectrum is normalized to the excitation light intensity, thanks to a beam splitter and a reference detector.

The absorption spectra of the scintillator mixture was measured using a Jasco V-760 Spectrophotometer provided with a LSE-701 Single Position Long Path Length (maximum: 100 mm) Cell Holder.

The absorption of the scintillator mixture was measured with respect to a blank obtained with hexane.

3.2. Measurements

We measured the emission spectrum of the JUNO liquid scintillator between 250 nm and 600 nm. The resulting spectrum is visible (in black) in figure 1. In the same figure are visible the emission spectra of pure LAB (in blue), of LAB + 2.5 g/L PPO (in red) and of LAB + 0.1 g/kg bis-MSB (in green). All of the spectra in figure 1 are normalized to the maximum to better appreciate the differences in their shape. The peak at 265 nm is caused by diffusion of incident light

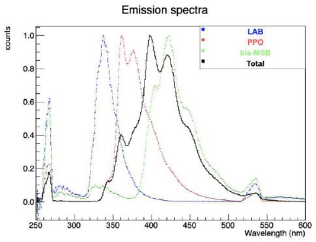

Figure 1: Emission spectra of the scintillator mixture and of its components.

and the peak at 530 nm is due to the second harmonic present in the beam of incident light.

As of today, this is the first measurement of the emission spectrum of the JUNO liquid scintillator mixture. This spectrum is very similar to the emission spectrum of bis-MSB, however, some other peculiar features are present at 400 nm and below. In particular, the peak at 400 nm is relatively more important in this spectrum and other two lower peaks are present at about 340 nm and 360 nm that are not visible in the bis-MSB emission spectrum. The peak

The peak at about 280 nm, due to light emission by LAB, vanishes when PPO is present in the mixture because of absorption by PPO. The structure between 320 nm and 350 nm in the spectrum of the mixture composed by LAB + 0.1 g/kg bis-MSB (in green in figure 1) is a residual of light emission by LAB, partly absorbed by bis-MSB.

The peak at 530 nm in all spectra correspond to the second harmonic in the excitation beam and is not a feature of the scintillator.

We measured the absorption spectrum of different samples, as reported in figure 2: pure LAB (in blue), LAB + 2.5 g/L PPO (in red), LAB + 0.1 g/kg bis-MSB (in green) and the mixture that will be used in JUNO, LAB + 2.5 g/L PPO + 3 mg/L bis-MSB (in black). All of the absorption spectra in figure 2 have been shifted to have the same minimum.

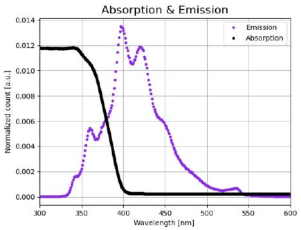

Figure 2: Absorption spectra of the mixtures.

We note that self-absorption of emitted light is non-negligible below 400 nm. This motivates the front-face method used for measurement of the emission spectrum, that would otherwise be affected by absorption, resulting both in a underestimation of the spectrum in the region at shorter wavelength and in a overestimation in the region at longer wavelength.

4. Timing properties

Once the emission and absorption spectra of the liquid scintillator are known, the timing properties can be investigated in a dedicated setup, using radioactive sources. Charged particles travelling in the scintillator do not only cause the emission of scintillation light, but can also cause the emission of Cherenkov light, depending on their velocity and the refractive index of the scintillator. If Cherenkov light is emitted, its contribution must be considered in the measurement of the timing properties of the scintillator. Here we describe the techniques that we used to separate and study the contribution of Cherenkov light thanks to its timing features.

The time distribution of fluorescence light emitted by the liquid scintillator is can be modeled with a superposition of different exponential distributions with characteristic time constants and relative weigth BIRKS (1964).

4.1. Setup

The setup for the measurement of the timing features of the light emitted by the liquid scintillator is basically composed by a cuvette made of optical glass filled with the liquid scintillator mixture and two PMTs facing the cuvette inside a black box. One PMT (model R1828-01) is part of an assembly (H1949-51) including a magnetic shield and faces the cuvette in close geometry, so that its optical coupling to the liquid scintillator is very strong. A second PMT (model R4220P) is a side-window PMT optimized for single-photon counting applications. This latter faces the cuvette in far geometry and different filters can be positioned between the cuvette and the PMT to further reduce the optical coupling to the liquid scintillator. To ensure the single-photon condition we always used a NDUV13A neutral density optical filter (optical density: 1.3).

The cuvette is enclosed in an aluminum frame and a cap closes its open face on top. The cap is provided with a needle that goes all the way into the liquid scintillator and allows nitrogen bubbling. Nitrogen bubbling has proven to be effective in reducing quenching caused by oxygen dissolved in liquid scintillators Lombardi et al. (2013). Gaseous nitrogen comes to the needle from a small tube provided with an entrance valve, bubbles in the liquid scintillator and gets out of the cuvette passing through a small hole and a tube with an exit valve.

The blackbox is positioned between two plastic scintillator modules placed immediately above and below the blackbox to veto the events caused by cosmic-ray induced muons passing through them. Each module is composed by a slab of EJ-200 (500 mm × 500 mm × 20 mm) wrapped in reflective foil, enclosed in a black vinyl light-tight container and coupled to a 25 mm PMT at one angle.

Signals coming from the PMTs facing the liquid scintillator are digitized by 2 separate NI PXIe-5162 digitizers (10 bit, 5 GS/s, 1.5 GHz) included in a NI PXIe-1075 chassis controlled by a NI PXIe-8135 embedded controller. Signals coming from the veto modules pass through a NIM coincidence unit whose output is digitized by a third NI PXIe-5162. The digitizers are operated in interleaving mode to fully exploit their capabilities and use the highest possible sampling rate.

4.1.1. *Impulse Response Function*

The Impulse Response Function (IRF) of the entire system has been measured using a pulsed laser source with 75 ps pulse width and a wavelength of 405 nm. The laser was coupled to an optical fiber entering the black box, terminated with a Teflon diffuser. The light scattered from the diffuser, conveniently attenuated by means of some optical filters, mimicks the emission from the scintillator and is sufficiently faint to fulfill the single-photon condition in the weakly-coupled PMT, yet sufficiently bright to cause the strongly-coupled PMT to trigger the acquisition. To better emulate the effect of refraction and reflections, the diffuser was placed inside a cuvette containing pure LAB and covered with an aluminum foil, so that the conditions were as close as possible to the real measurement 3a. Considered the dead time of the digitizers, the period of the laser (20 μs) has been chosen to have the highest counting rate.

We measured the IRF placing the diffuser in three different positions inside the cuvette to study the different effect of refraction and reflections 3b.

The IRF has been fitted using a superposition of 7 Gaussian distributions, which is a reasonable trade-off between the most simple and the most accurate description of its different features.

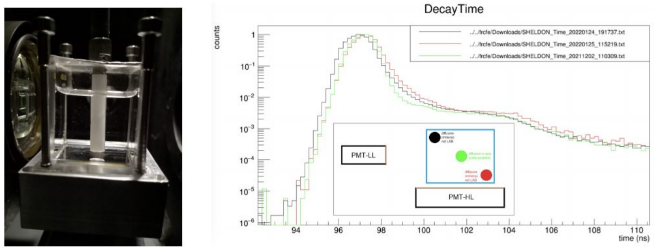

(a) Beta

(b) Alpha

4.2. Measurement of the fluorescence time distribution

The time distribution of the fluorescence light emitted by the scintillator can be described by the superposition of some exponential distributions. Given our 1600 ns long acquisition window, we modeled the time distribution of emitted light with four effective components. Such a choice has already been motivated in previous literature, which mostly describes the LAB-based scintillators with four exponential components **?**. Thanks to the high resolution of our setup, we were able to observe the rising edge of the light signal and this had to be taken into account in our analysis. The resulting distribution can be written as

$$F_{fit} = N\sum_{d=1}^{4}\frac{q_d}{\tau_d-\tau_r}\left(e^{-\frac{t-t_0}{\tau_d}}-e^{-\frac{t-t_0}{\tau_r}}\right)\Theta(t-t_0) \quad (1)$$

where N is a normalization constant, q_d and τ_d are the relative weights (also called fractions hereafter) of the d-th component and its characteristic decay times, τ_r is the characteristic rise time (common to all the four components) and Θ is the step function that marks the start of the fluorescence time profile. The normalization of the fourth component requires a particular treatment due to the acquisition time window, which is limited to 1.6 μs. This limitation implies a truncation in the light collection, so the normalization of the fourth exponential component $\frac{1}{\tau_4-\tau_r}$ needs to be corrected:

$$q_4 = \frac{1-\sum_{d=1}^{3} q_d}{1-e^{-\frac{t_w-t_0}{\tau_4}}} \quad (2)$$

where t_w = 1600 ns is the length of the DAQ time window. The light uncollected because of the finite duration of our acquisition window is about 9.1% of the fourth component

To take into account the finite resolution of the setup it is necessary to convolve the fluorescence model described in equation 1 with the IRF:

$$(f*g)(t) = \int_{-\infty}^{\infty} f(\tau)g(t-\tau)d\tau \quad (3)$$

Thanks to the linearity of the operation, the analytic convolution of the IRF with the fluorescence model in equation 1 gives

$$F_{fluo}(t) = N\sum_{d=1}^{4}\sum_{j=1}^{7} N_d N_j\left(e^{-t/\tau_d}-e^{-t/\tau_r}\right) * G_j(t;\mu_j,\sigma_j) \quad (4)$$

where the N_d is the normalization of the fluorescence component, as discussed before, the N_j are the normalized weights of the seven Gaussian functions and N is the total number of entries in the histogram.

Cherenkov radiation is emitted with characteristic time shorter than the resolution of our setup so we model it as an impulse distribution. Also the Cherenkov contribution has to be convolved with the IRF and the time distribution of emitted light is a weighted sum of fluorescence 1 and Cherenkov light:

$$F_{Total}(t) = \left[N_{Ch}\,\delta(t,t_0) + (1-N_{Ch})\,F_{Fluo}(t)\right] * \mathrm{IRF}(t) \quad (5)$$

where N_{Ch} is the fraction of Cherenkov light with respect to total emission (Cherenkov and fluorescence).

4.3. Uncertainties

5. Pulse Shape Discrimination

6. Conclusions

Acknowledgements

7.

References

Beretta, M., 2022. Improved measurement of timing and optical properties of the JUNO scintillator. Master's thesis. Univeristy of Milan.

BIRKS, J., 1964. Chapter 8 - organic liquid scintillators, in: BIRKS, J. (Ed.), The Theory and Practice of Scintillation Counting. Pergamon. International Series of Monographs in Electronics and Instrumentation, pp. 269–320. URL: https:

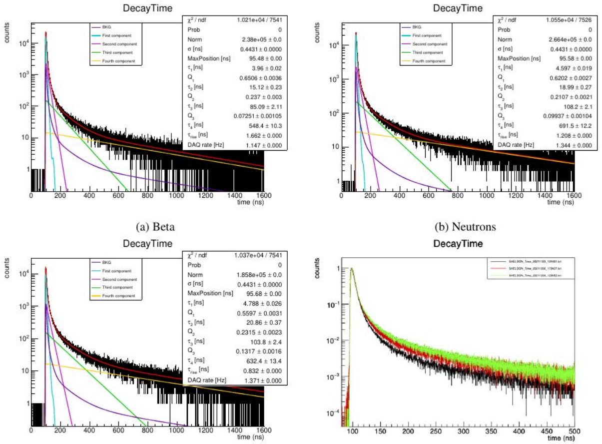

(a) Beta (b) Neutrons

(c) Alpha (d) Caption

Figure 4: Caption

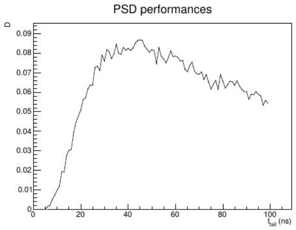

Figure 5: BlaBla

//www.sciencedirect.com/science/article/pii/B9780080104720500136, doi:https://doi.org/10.1016/B978-0-08-010472-0.50013-6.

Knoll, G.F., 2018. Radiation detection and measurement, 4^{th} ed. WILEY.

Lombardi, P., Ortica, F., Ranucci, G., Romani, A., 2013. Decay time and pulse shape discrimination of liquid scintillators based on novel solvents. Nuclear Instruments and Methods in Physics Research Section A: Accelerators, Spectrometers, Detectors and Associated Equipment 701, 133–144. URL: https://www.sciencedirect.com/science/article/pii/S0168900212012077, doi:https://doi.org/10.1016/j.nima.2012.10.061.

To be concluded very soon…

Thank you
Questions?

Backup

Cosmic background in SHELDON

DAQ screenshot during the measurement

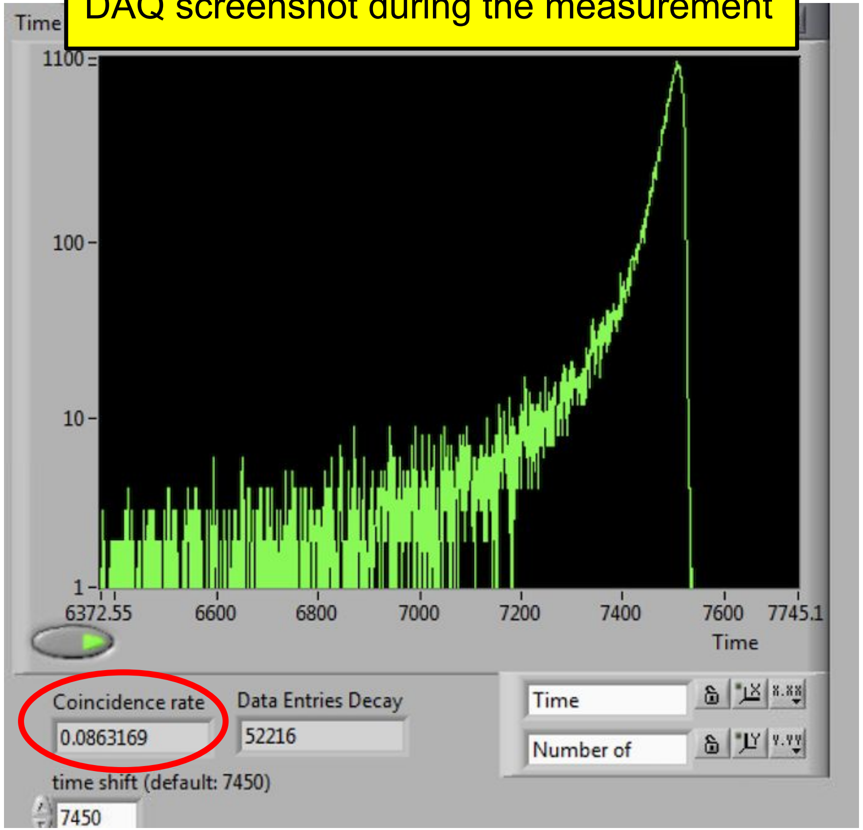

We have measured the rate of cosmic muons detected by our setup **without any radioactive source**

We have determined the fluorescence parameters associated to this distribution

Monte Carlo study

Cosmic background

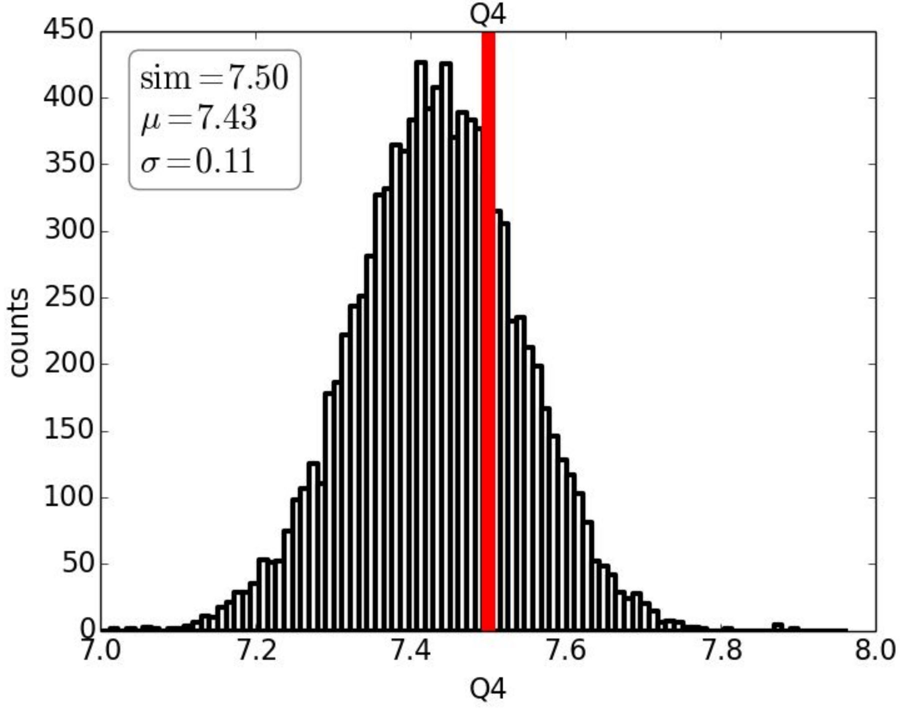

Reconstruct Q4 parameter in a alpha measurement comparing to **injected value**

We have measured the rate of cosmic muons detected by our setup **without any radioactive source**

We have determined the fluorescence parameters associated to this distribution

We have evaluated the impact of this background in our measurement using simulations

Fit model: Cherenkov contribution

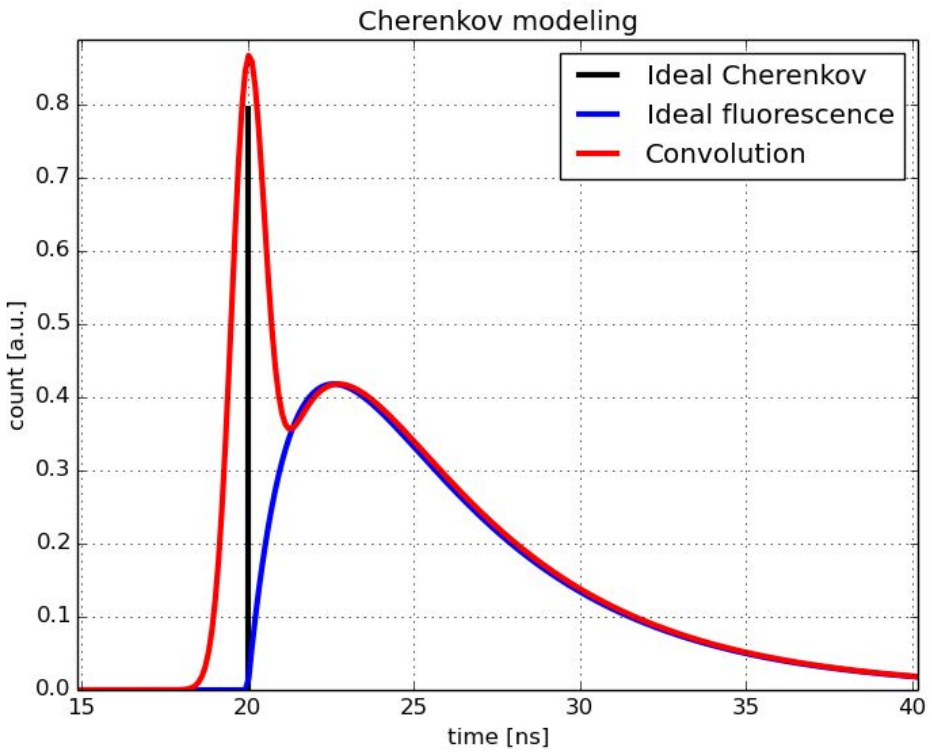

The Cherenkov contribution is modeled as a **delta function**

It is summed to the **fluorescence** model

The **sum** is convolved with the detector response

$$\mathrm{IRF}(t) = \sum_{j=1}^{7} N_j \, G_j(t; \mu_j, \sigma_j)$$

$$F_{Total}(t) = [N_{Ch} \, \delta(t, t_0) + (1 - N_{Ch}) \, F_{Fluo}(t)] * \mathrm{IRF}(t)$$

Cherenkov contribution at different wavelengths

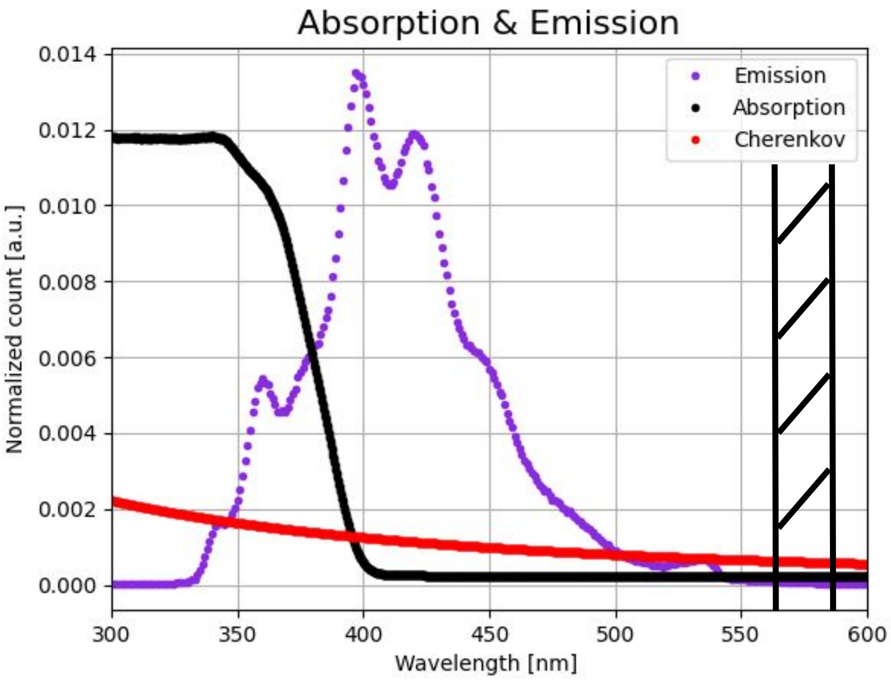

580 - 10 nm

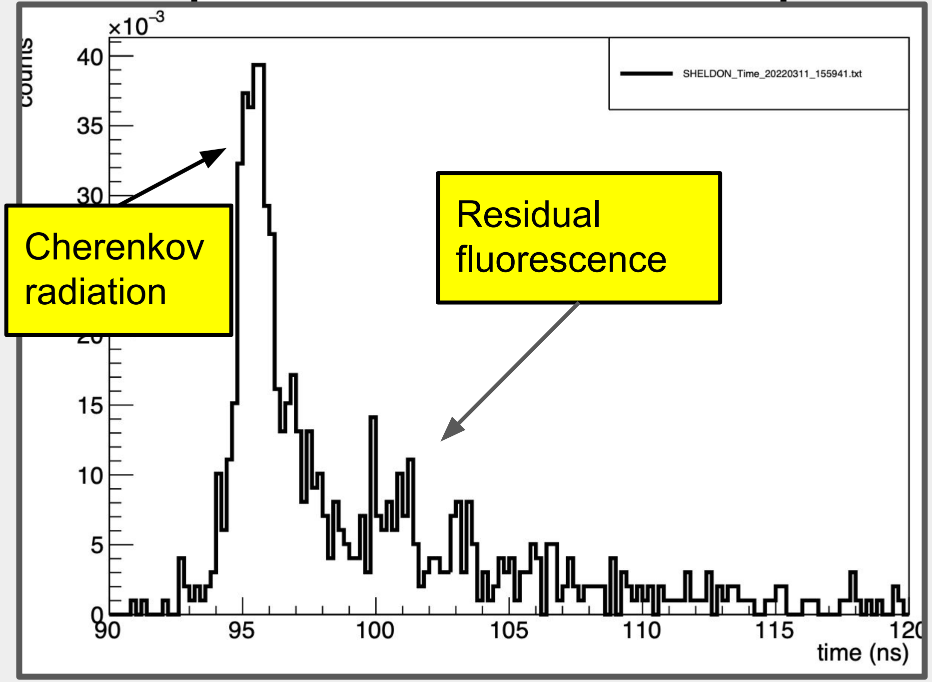

Cherenkov ≥ 25 %

Cherenkov contribution at different wavelengths

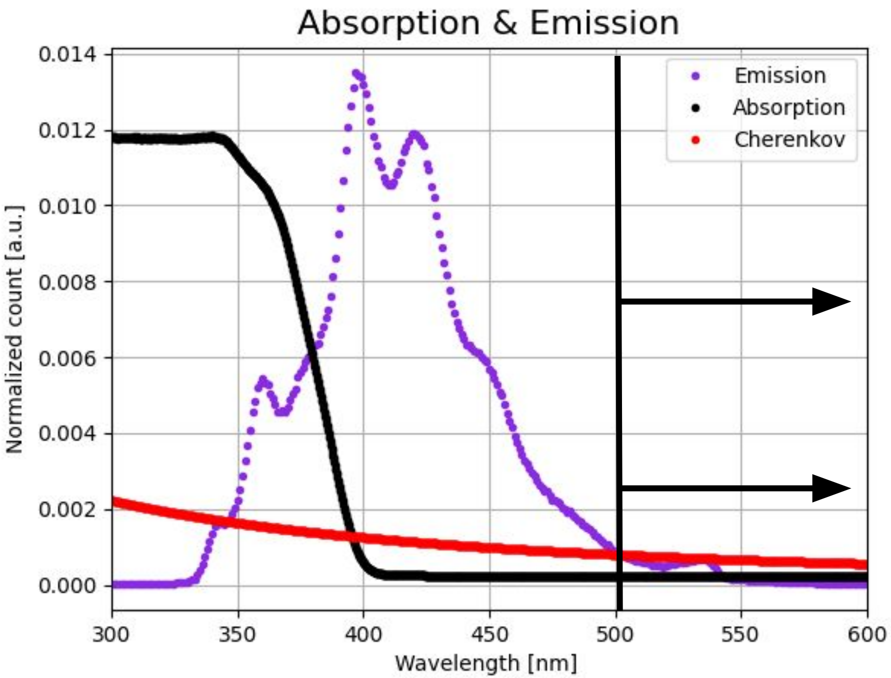

500 nm pass long filter

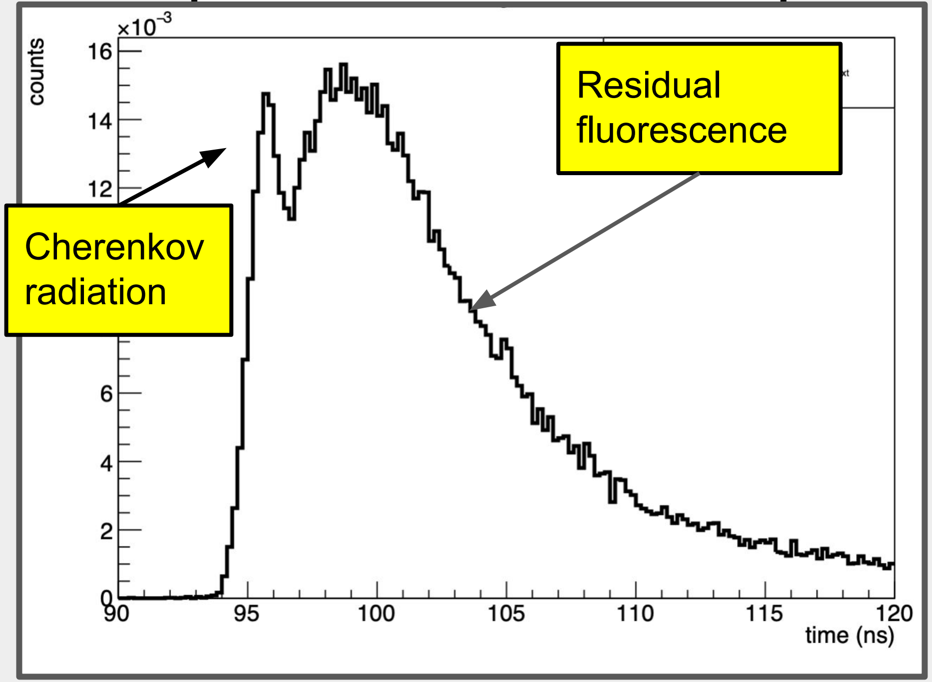

Cherenkov = 8.56 ± 0.16 %

The SHELDON project: Impulse Response Function

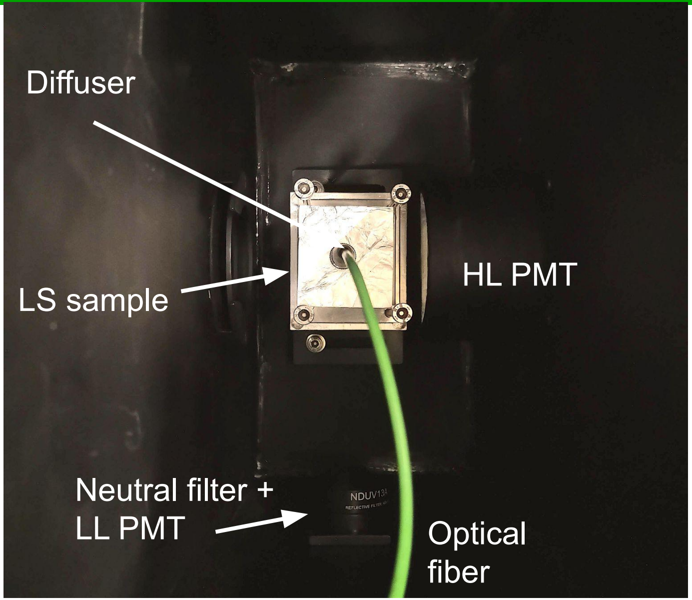

The measurement of the Impulse Response Function is performed using a laser.

The laser has a pulse duration of 75 ps.

A diffuser is placed at the end of the optic fibre to mimic a point like emission

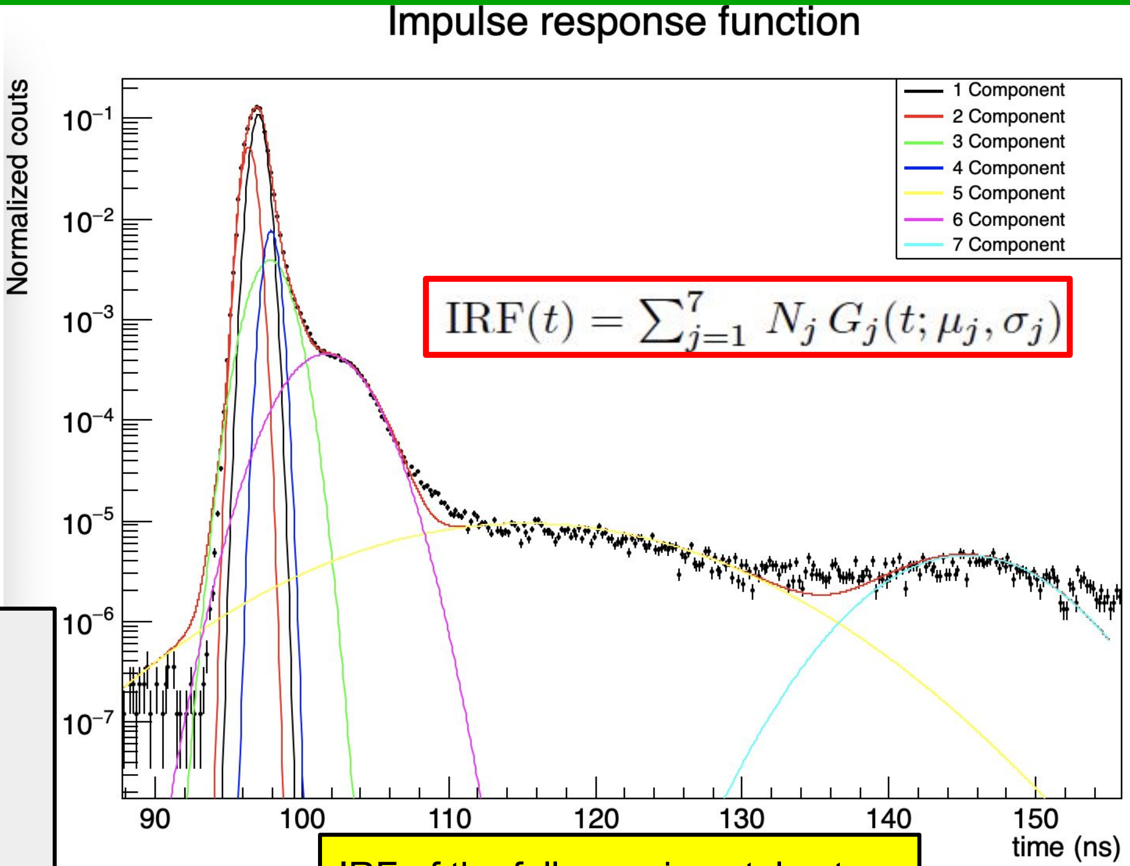

IRF of the full experimental setup:
LS + PMT + ADC + CFD

Method validation

Monte Carlo simulation to produce **10^4 fake datase**t
used to evaluate the **possible fit sistematics** on fluorescence parameters

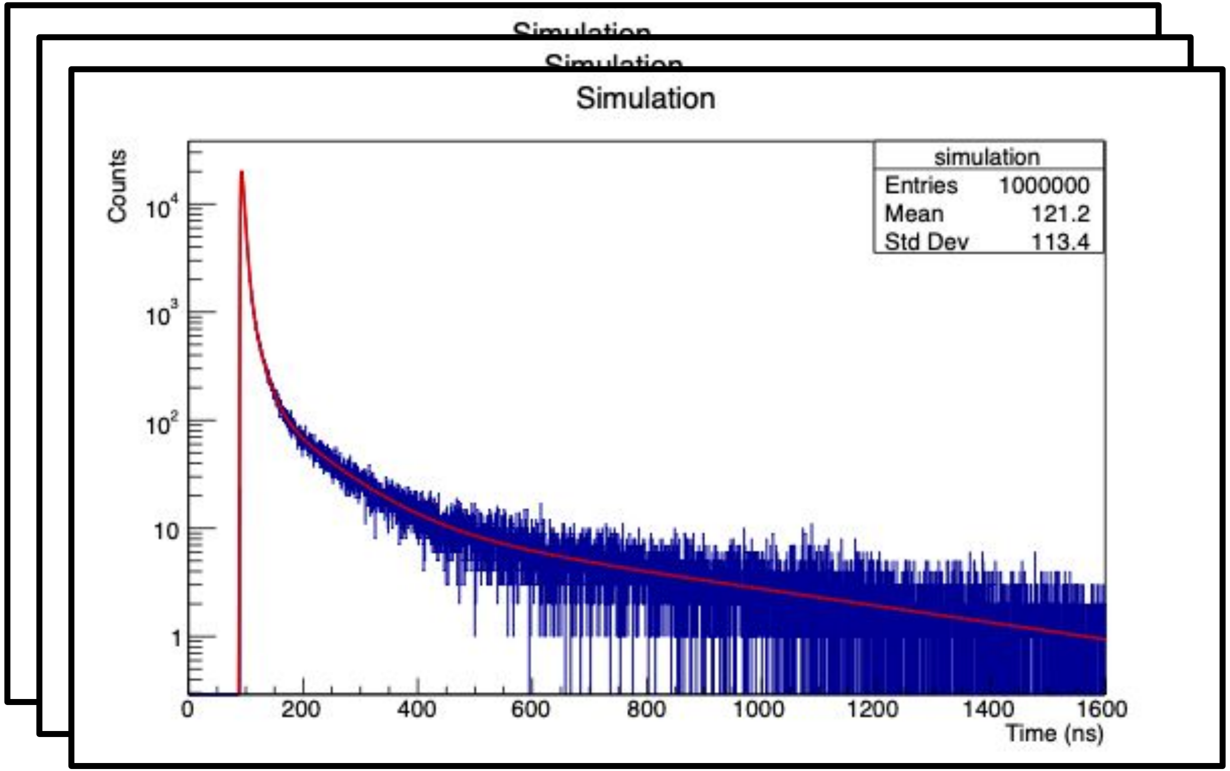

marco.beretta@unimi.it

Monte Carlo study

Method validation

The uncertainties on the fluorescence parameters are at the percentage level

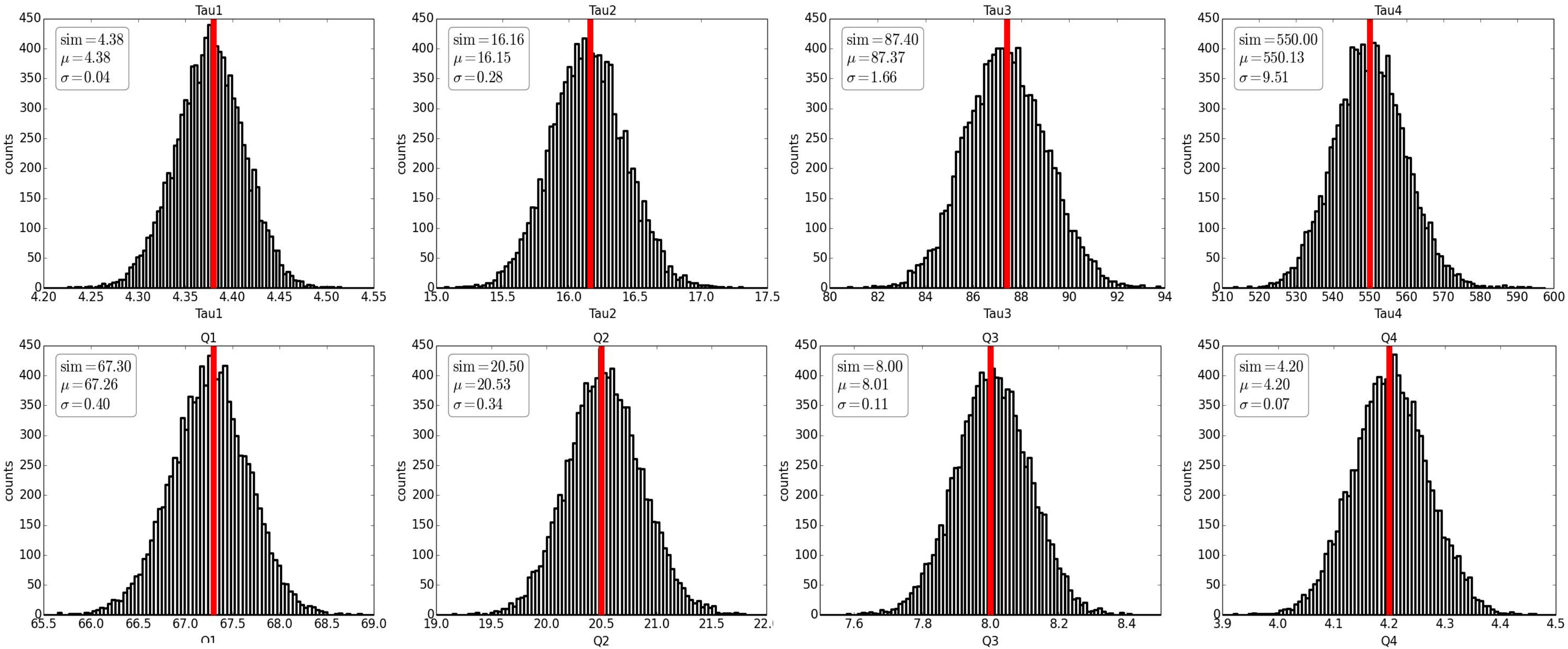

No relevant bias is shown on all parameters

marco.beretta@unimi.it

Monte-Carlo study

Systematic error introduced by the choice the DAQ time window

The relative uncertainty on slow component decreases as the upper end of the DAQ time window increases.

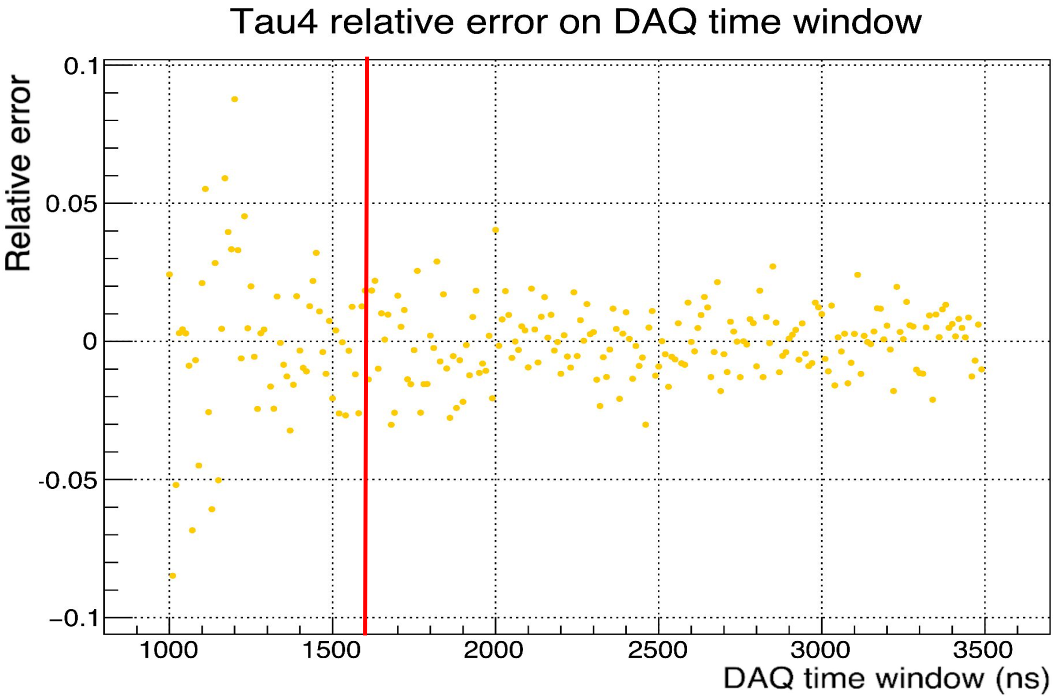

The red line represent our DAQ time window

The number of events is fixed (similar to a measurement lasting **one week**)

As the statistic increases the uncertainty decreases

The trend does not change with increasing statistics

marco.beretta@unimi.it

Measurement of fluorescence: Results

	τ_1 [ns]	τ_2 [ns]	τ_3 [ns]	τ_4 [ns]	τ_r [ns]
α	4.79 ± 0.02	20.86 ± 0.39	103.8 ± 2.4	633 ± 14	0.832 ± 0.002
p	4.60 ± 0.02	18.99 ±0.27	108.2 ± 2.1	691 ± 12	1.208 ± 0.001
e^-	3.96 ± 0.02	15.11 ± 0.22	85.0 ± 2.0	549 ± 9	1.667 ± 0.001
	q_1 [%]	q_2 [%]	q_3 [%]	q_4 [%]	χ^2_r
α	55.97 ± 0.32	23.15 ± 0.23	13.17 ± 0.16	8.50 ± 0.42	1.38
p	62.02 ± 0.27	21.07 ± 0.21	9.94 ± 0.10	6.97 ± 0.36	1.4
e^-	65.02 ± 0.36	23.72 ± 0.28	7.26 ± 0.10	4.27 ± 0.47	1.35

PRELIMINARY RESULTS ON THE JUNO MIXTURE

marco.beretta@unimi.it

Measurement of fluorescence: Results

Particles	Fast(ns)/ Ratio	Slow(ns)/ Ratio	Slower(ns)/ Ratio	Slowest(ns)/ Ratio
γ, e^+, e^-	4.6/70.7%	15.1/20.5%	76.1/6.0%	397/2.8%
n, p^+	4.5/61.4%	15.7/23.2%	76.2/9.0%	367/6.4%
α	4.345/49.82%	17.64/27.39%	89.045/14.67%	544.48/8.12%

Talk of Yaoguang Wang “Detector simulation status” 18/07/2022

e^-	3.96/65.02%	15.11/23.72%	85.0/7.26%	549/4.27%
p	4.60/62.02%	18.99/21.07%	108.2/9.94%	691/6.97%
α	4.79/55.97%	20.86/23.15%	103.8/13.17%	633/8.50%

Determination of the Cherenkov spectrum

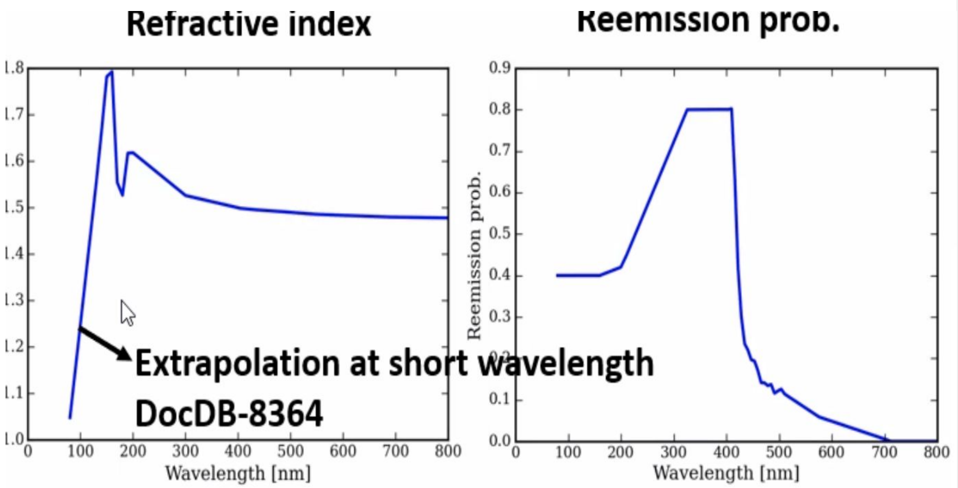

Talk of Yaoguang Wang “Detector simulation status” 18/07/2022

Using the new measurement of the **refractive index**

$$\frac{\partial^2 E}{\partial x \partial \omega} = \frac{q^2}{4\pi}\mu(\omega)\omega\left(1 - \frac{1}{\beta^2 n^2(\omega)}\right)$$

marco.beretta@unimi.it

Systematic error introduced by fit ⟶ 7 Gaussians

The modeling of the time rensonse affects more on the 1[nd] and the 2[nd] component

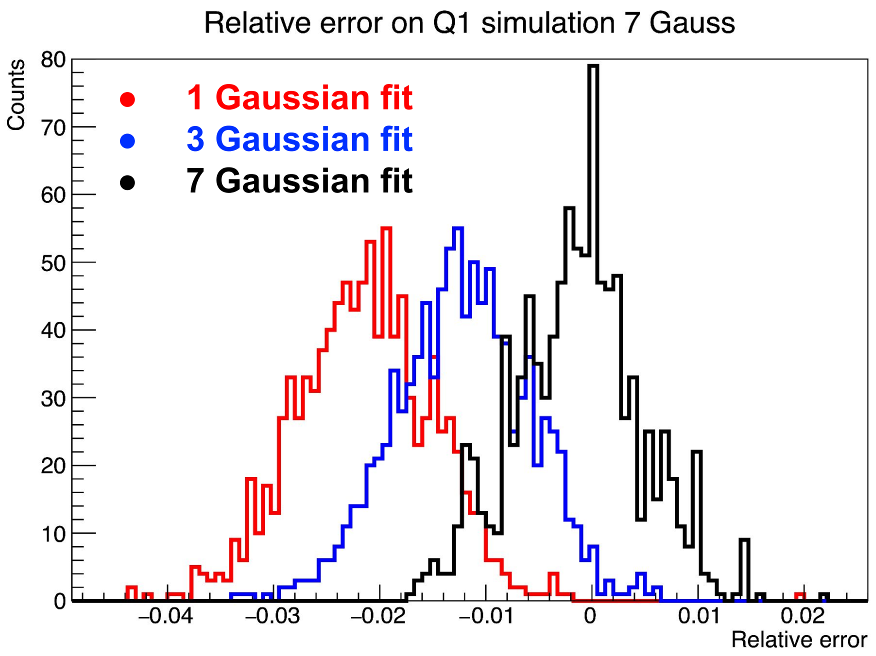

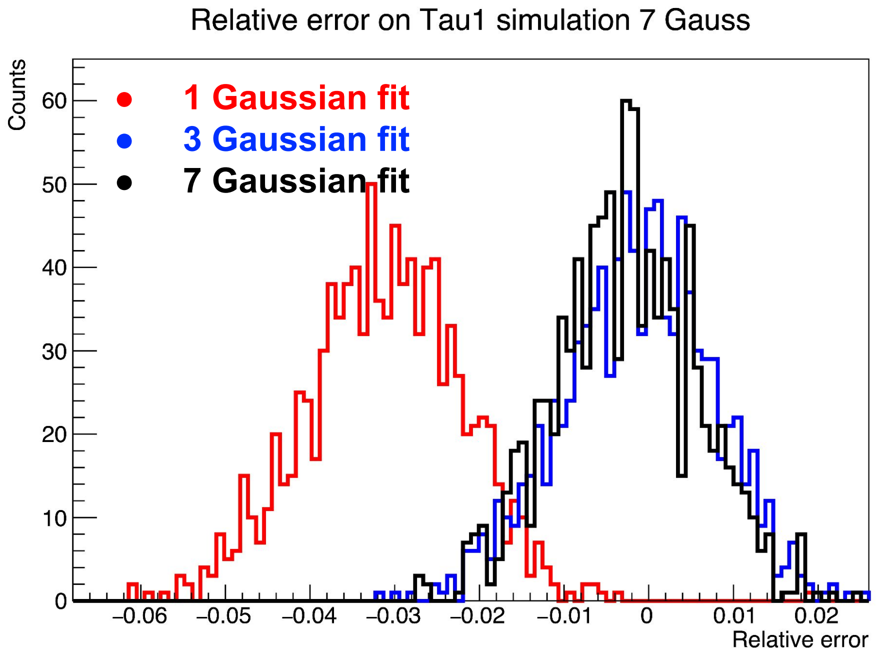

marco.beretta@unimi.it

Measurement of fluorescence time profile with the single photon counting technique

Time-correlated single photon counting (TCSPC) is a technique to measure the fluorescence decay time.

Under certain hypothesis (R_{sp}<<R_{tr}), the time of arrival of the photons w.r.t. to the trigger reproduces the fluorescence time distribution.

In our application, one PMT provides the START signal (trigger) and the other PMT gives the STOP signal.

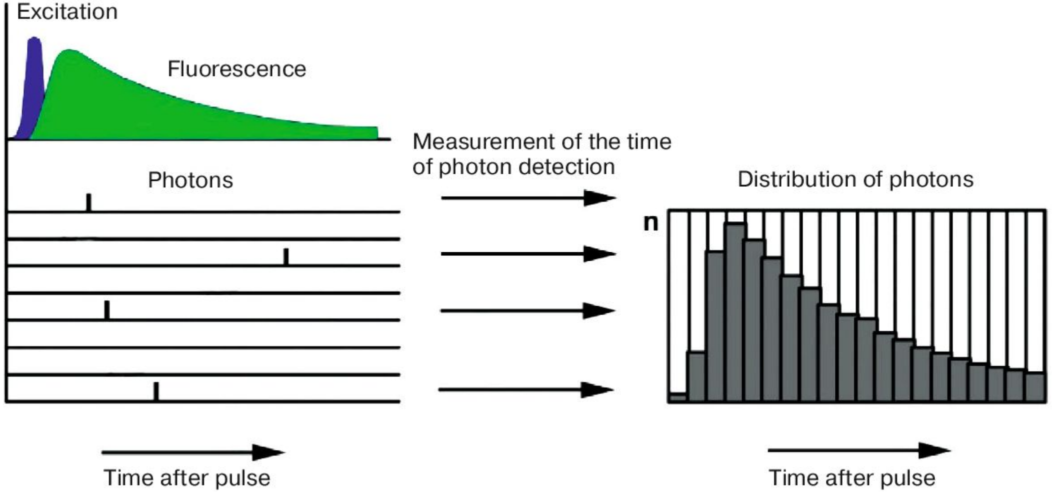

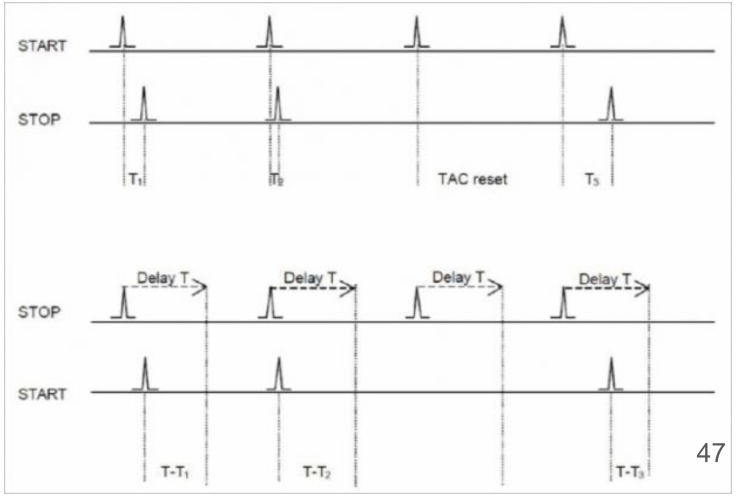

Monte-Carlo study

Systematic error due to the exclusion of the Cherenkov contribution in the fit ⟶ Cherenkov **not** included

The exclusion of Cherenkov light on the fit mostly affects on the fast component

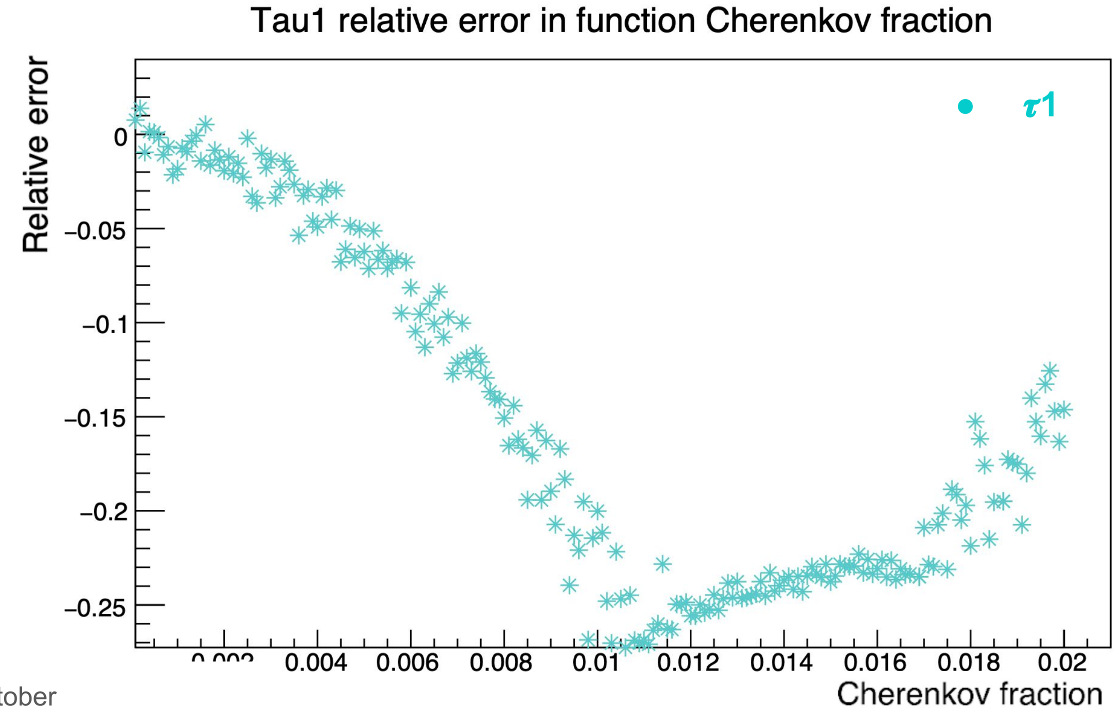

Monte-Carlo simulates different contribution of Cherenkov light

The fit does not consider the Cherenkov light

marco.beretta@unimi.it

Monte-Carlo study

Systematic error due to the exclusion of the Cherenkov contribution in the fit ⟶ Cherenkov **not** included

The exclusion of Cherenkov light on the fit mostly affects on the fast component

Tau1 relative error in function Cherenkov fraction

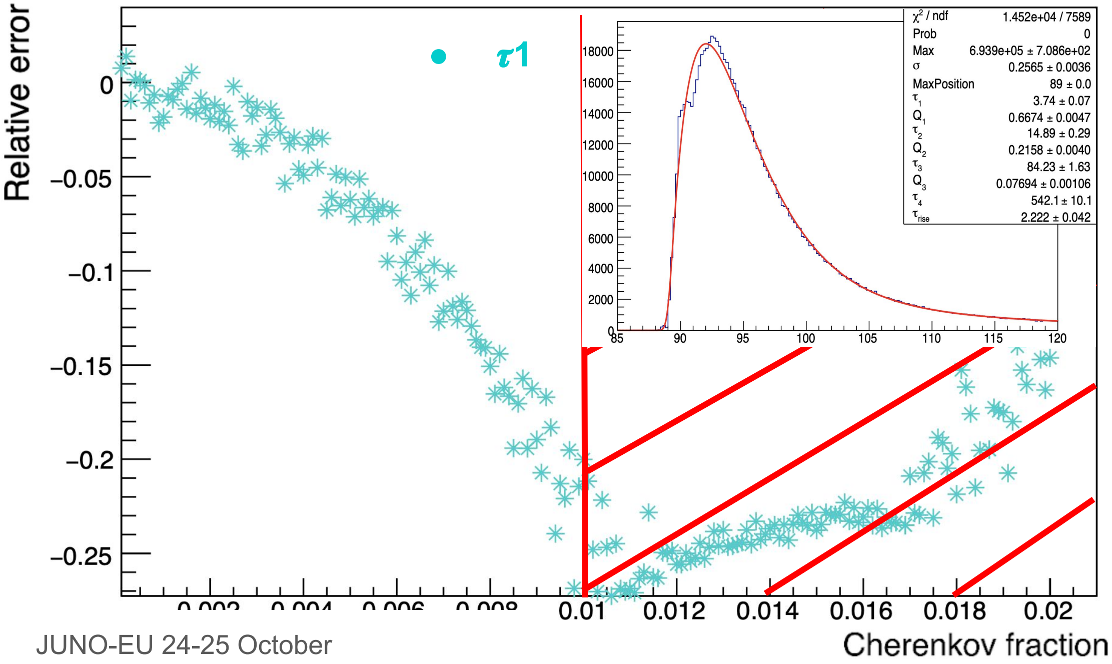

The part of the graph above 0.01 fraction makes no sense. In that case Cherenkov light becomes important and the fit doesn't work.

The relative error gets worse as the Cherenkov fraction increases

marco.beretta@unimi.it

Monte-Carlo study

Systematic error due to the exclusion of the Cherenkov contribution in the fit ⟶ Cherenkov **not** included

The exclusion of Cherenkov light on the fit mostly affects on the fast component

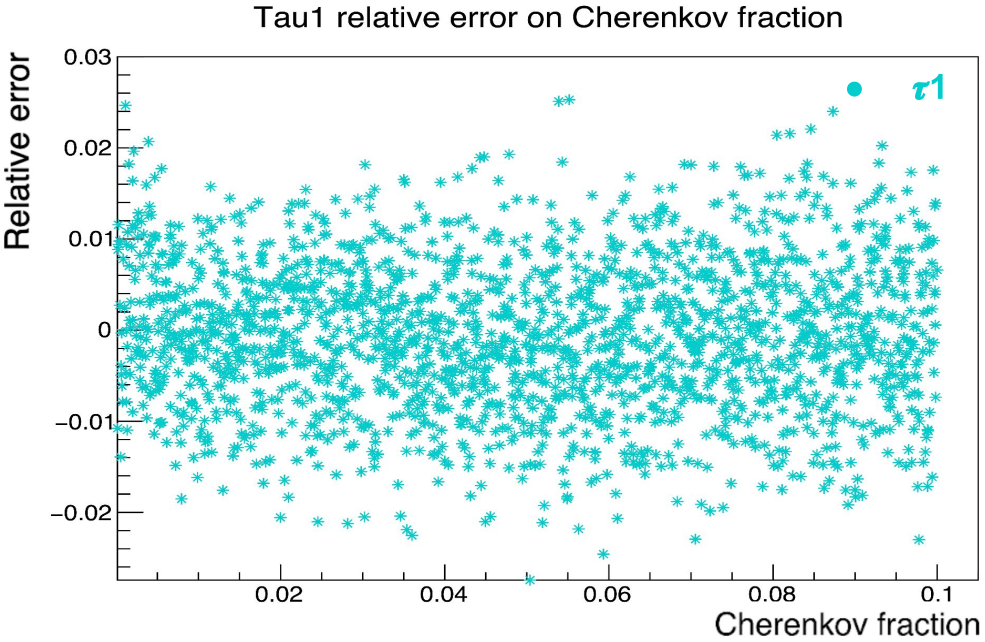

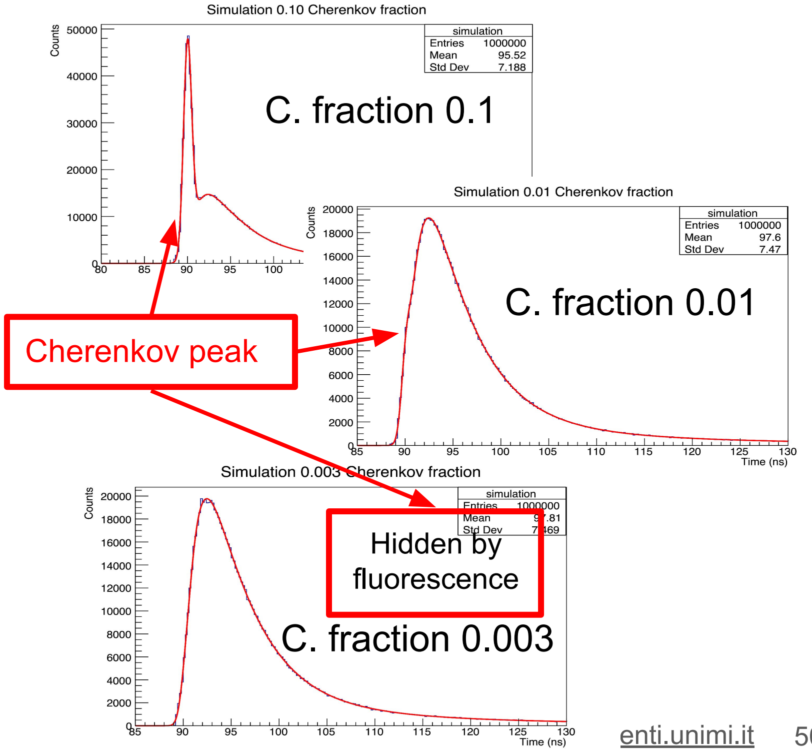

Monte Carlo study

Systematics studies: Cherenkov neglect

Same **Monte Carlo simulation** of the sensitivity studies

Cherenkov **simulated** in the time distribution, but **neglected in the fit**

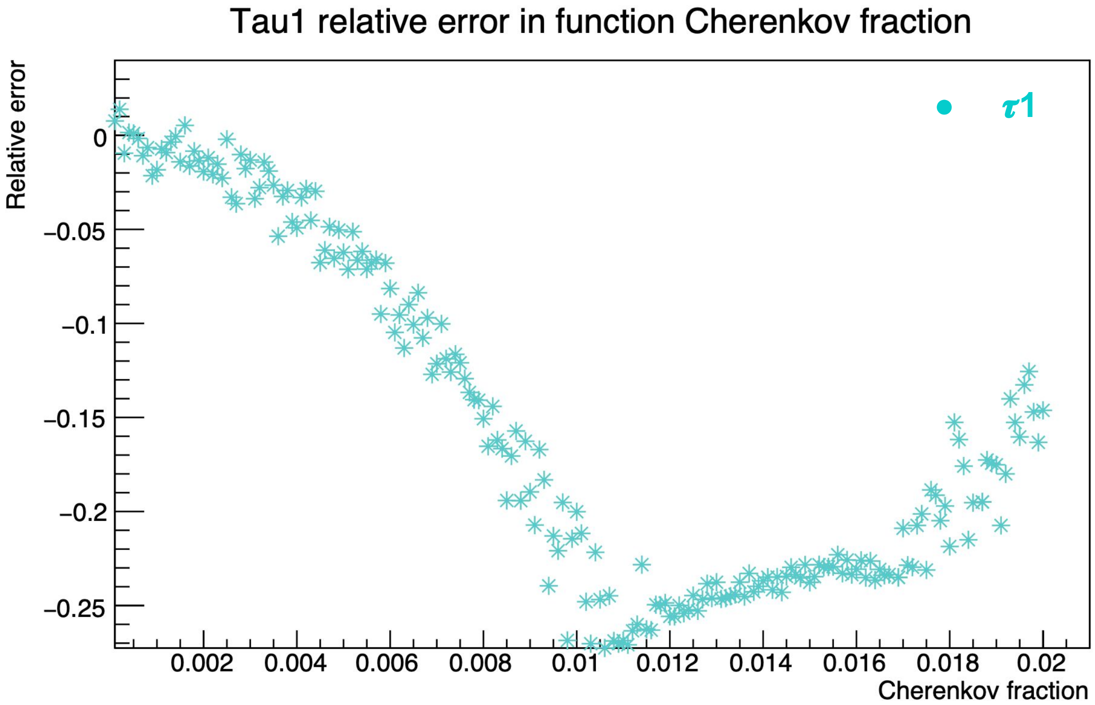

marco.beretta@unimi.it

Systematics studies: Cherenkov neglect

Same **Monte Carlo simulation** of the sensitivity studies

Cherenkov **simulated** in the time distribution, but **neglected in the fit**

Tau1 relative error in function Cherenkov fraction

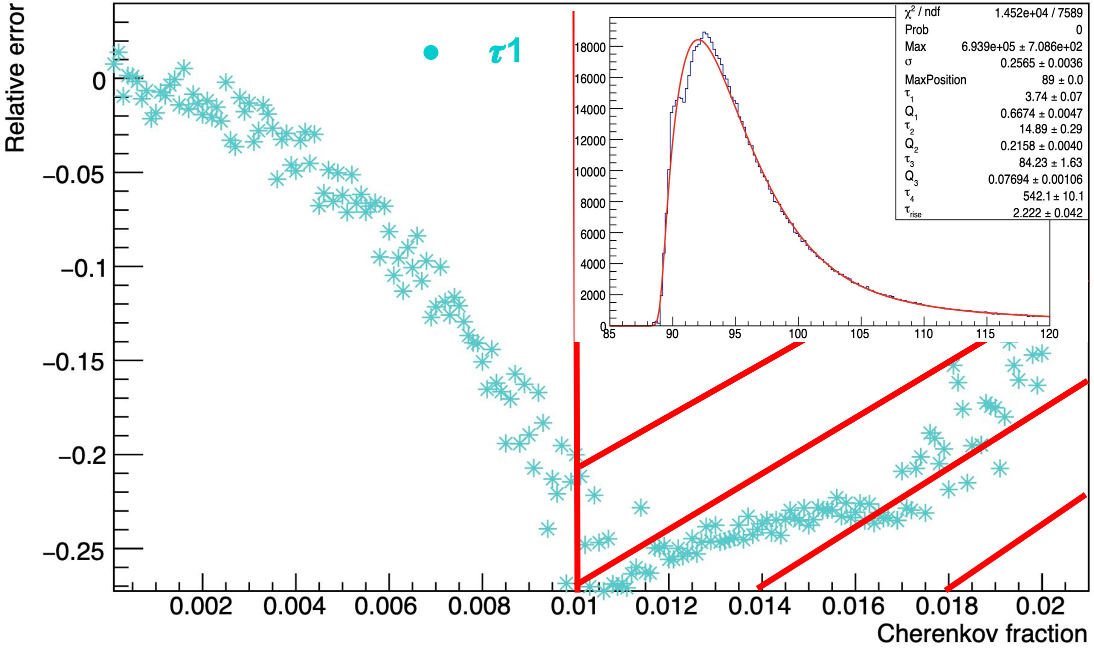

The part of the graph above 0.01 fraction makes no sense. In that case Cherenkov light becomes important and the fit doesn't work.

The relative error gets worse as the Cherenkov fraction increases

marco.beretta@unimi.it

Monte-Carlo study

Cherenkov sensitivity study

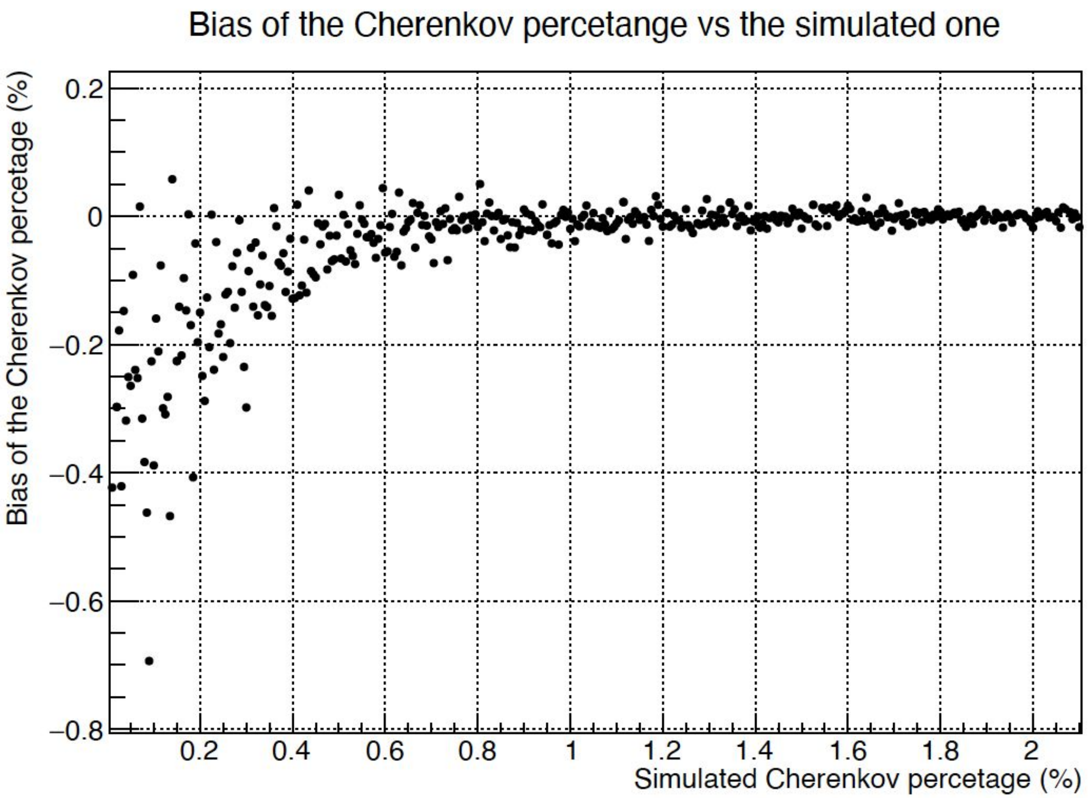

marco.beretta@unimi.it

Normalization of the fourth component

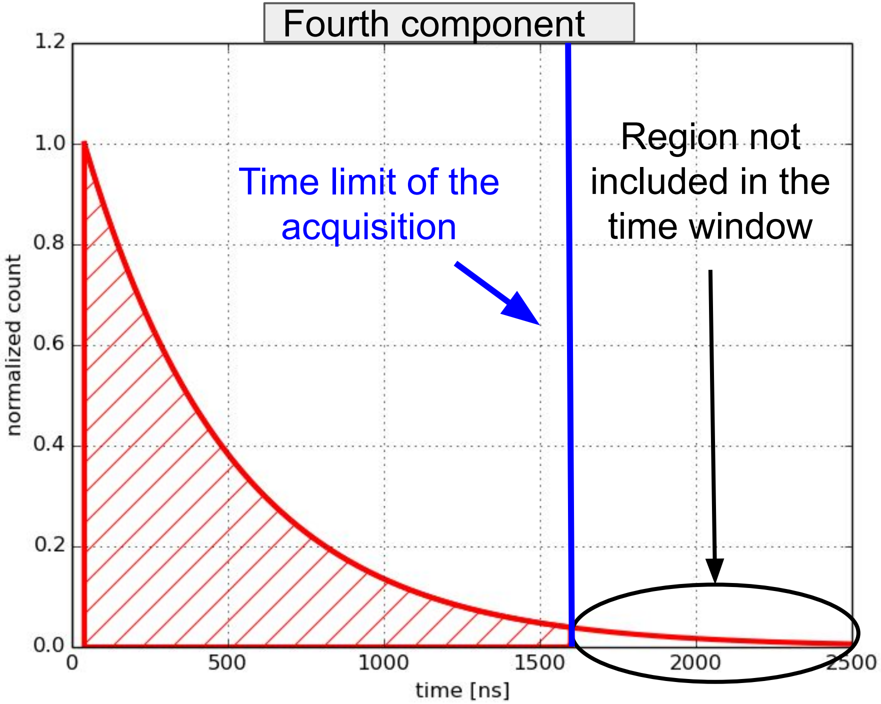

The fit model uses four components to describe the de-excitation time of the L.S.

These components are normalized to the integral of the exponential

For the fourth component this introduces an error

We improve the implementation of this normalization to consider this error

marco.beretta@unimi.it

Monte-Carlo study

Systematic error introduced by fit ⟶ On 10^5 simulations

A simple Monte Carlo was realized to study the fit systematics.

The percentage uncertainty introduced by the fit is less than 5% on τ_i and q_i.

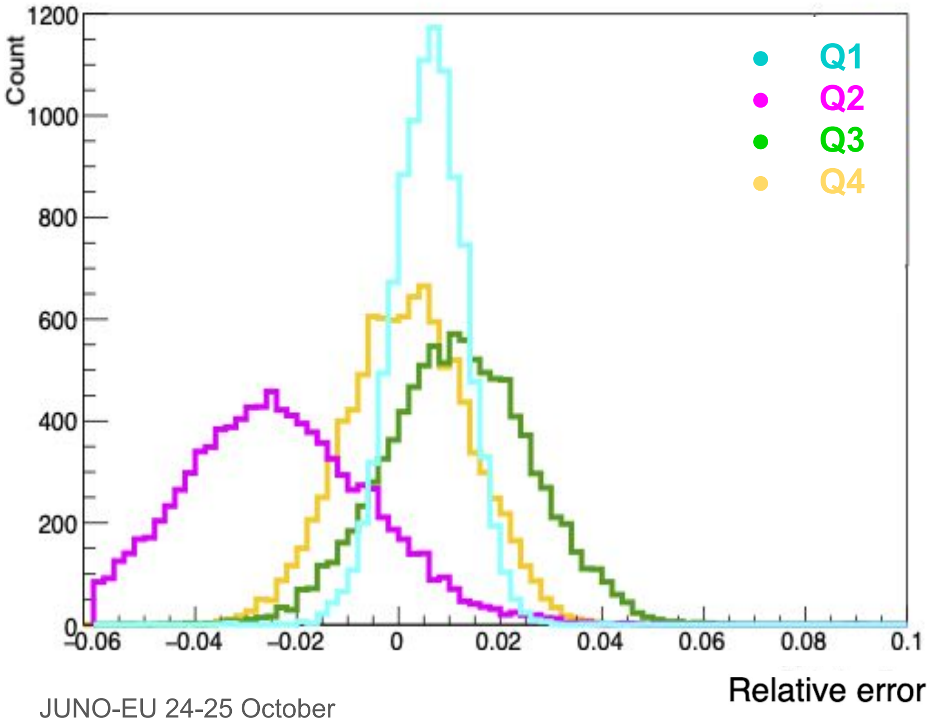

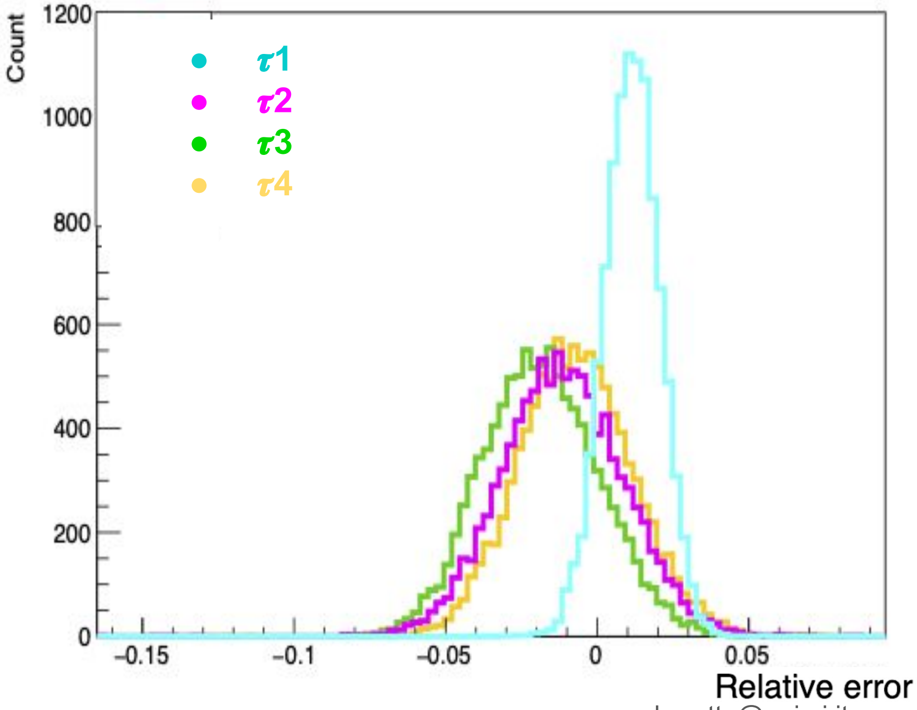

marco.beretta@unimi.it

Monte-Carlo study

Systematic error introduced by a different description of the detector response

Only 1 Gaussian was used instead of 3 to describe the system response

In this case the percentage uncertainty gets worse for the fast component

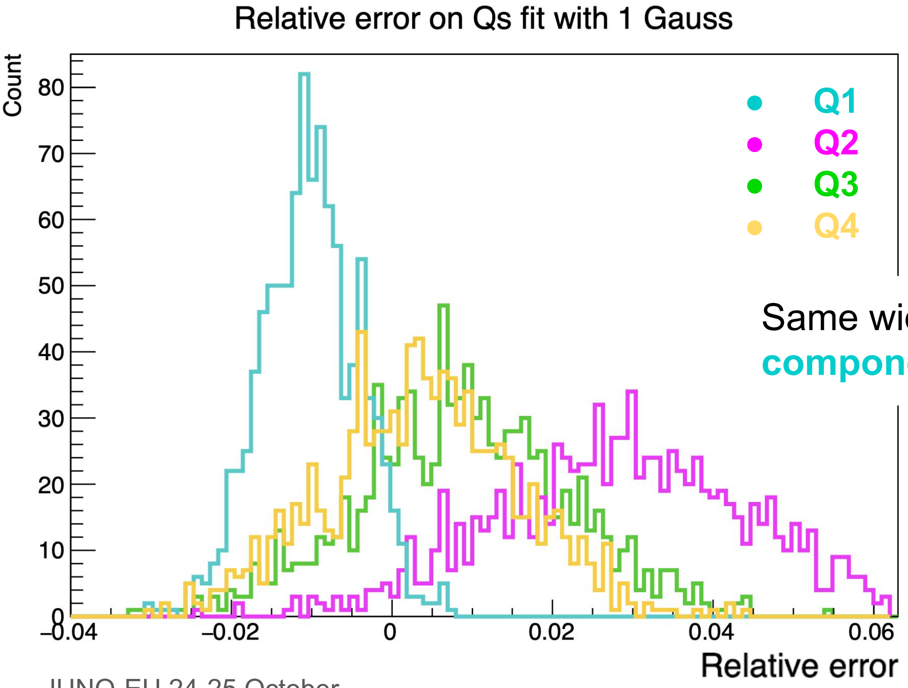

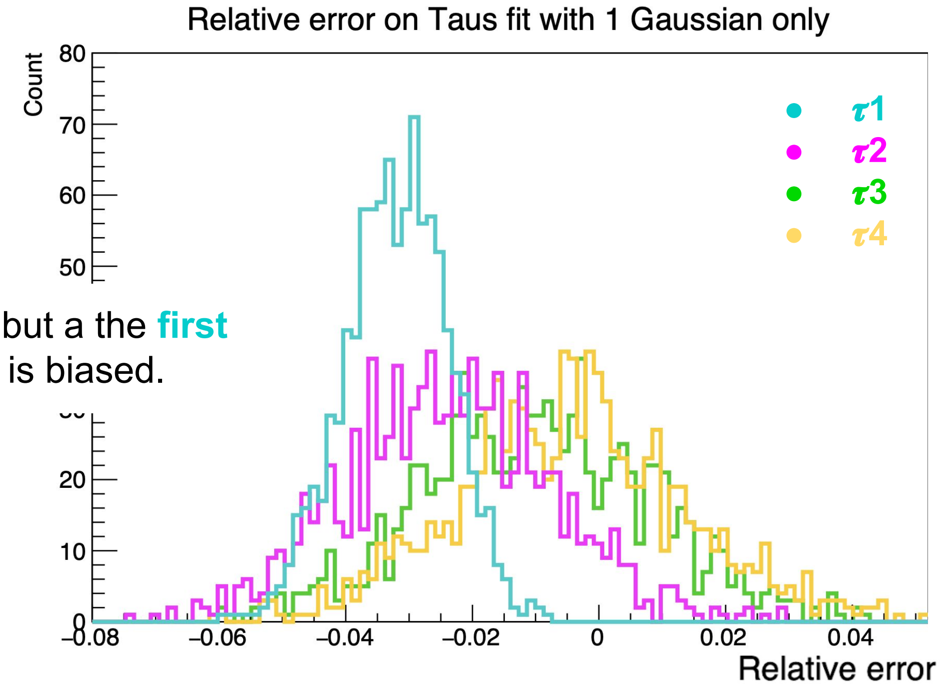

Same width but a the **first component** is biased.

marco.beretta@unimi.it